

1 **HESS 2015-325 author responses and revisions to F. Painosi’s report submitted April 28,**  
2 **2016**

3 **“Parameter regionalization of a monthly water balance model for the conterminous United**  
4 **States”**

5 **Andrew Bock, [abock@usgs.gov](mailto:abock@usgs.gov)**

6 **Note:** line numbers/page numbers for author’s response to comments are based on the latest  
7 uploaded manuscript (5/25/2016).

8 • **Reviewer comment #1 (marked by comment *Bock1* in this version of manuscript):**

9 Lines 215-217: "For our application we generated an ensemble of 1000 parameter sets (as  
10 compared to the minimally suggested number of 71 estimated by ‘fast’) to have the  
11 capability to have the capability to compare results of different sensitivity analysis  
12 methods". Unclear. It seems to me that no other SA method was applied. The only reason  
13 I see here to increase the sample size is to increase the robustness of sensitivity estimates  
14 produced by FAST.

15 **Author’s response (marked by comment *Bock2* in this version of manuscript):** Yes

16 this is a good point that we didn’t make clear enough on the last version. While the  
17 number of parameter runs was not a time-restraint because of the simplicity of the  
18 MWBM, we modified this section to include this “robustness” reasoning suggested by  
19 the reviewer, and included a statement that the use of the minimal number of parameter  
20 sets should be a consideration for the application of FAST to more complex models (such  
21 as finer temporal resolution or larger number of parameters) .

22 **Changes in the text:**

23 Section 2.2: Fourier Amplitude Sensitivity Test

24 ○ Page 8, line 213: Removed the text "...to have the capability to compare results  
25 of different sensitivity methods."

26 ○ Page 8, lines 214-217: Added the following text:

27 "The use of the minimal number of parameter sets should be a consideration for  
28 more complex models, but the relative computational efficiency and  
29 parallelization of the MWBM allowed the model to be simulated with this larger  
30 number of parameter sets quickly to help ensure a robust parameter sensitivity  
31 analysis."

32

33 • **Reviewer comment #2 (marked by comment *Bock3* in this version of manuscript):**

34 Lines 252. "The following sections describe the parameter regionalization procedure in  
35 detail (Fig. 3)." Maybe worth inserting a short explanation of the key steps in the  
36 procedure? The Figure is helpful but not self-explaining.

37 **Author's response (marked by comments *Bock4* and *Bock5* in this version of**

38 **manuscript)** We have revised the opening paragraph of section 3, the figure caption for  
39 Figure 3, and Figure 3 itself to be more consistent with section names, section numbers,  
40 and the names of data objects, methods and objects used in this section.

41 **Changes in the text:**

42 Section 3: Parameter regionalization procedure

- 43           ○ Page 9, line 227-8: Added an introduction to the section that immediately links  
44           the sub-sections to the flow chart- “The following sections describe the workflow  
45           for the MWBM calibration and regionalization (illustrated in Figure 3).“
- 46
- 47           ○ Page 9, lines 230- Deleted “across the CONUS” for redundancy
- 48
- 49           ○ Page 9, lines 229-236: - Modified this section to explicitly use the sub-section  
50           names and numbers to describe the workflow:
- 51             
52           “The spatial patterns and magnitudes of parameter sensitivities were used to  
53           organize the 109,951 HRUs into hydrologically similar regions referred to in the  
54           paper as calibration regions. During the initial streamgage selection, potential  
55           streamgages were identified for use in the grouped MWBM calibration. These  
56           selected streamgages then were individually calibrated. Using a number of  
57           selection criteria, a final set of calibration gages were derived within each  
58           calibration region. The grouped MWBM calibration produced an ‘optimal’ set of  
59           MWBM parameters for each calibration region by evaluating simulated MWBM  
60           variables converted to Z-scores.”
- 61
- 62           ○ Page 9, lines 237-240 – Added detail to the figure caption to help link the figure  
63           back to the sub-sections of Section 3:
- 64           “Figure 3. Schematic flowchart of the parameter regionalization procedure  
65           described in Section 3: Parameter sensitivities (3.1), Calibration regions (3.2),  
66           Initial streamgage selection (3.3), and Grouped streamgage calibration (3.4).”

67  
68

69 • **Reviewer comment #3 (marked by comment *Bock6* in this version of manuscript):**  
70 Figure 5 (and comments on Lines 300-302): I am still not persuaded of this explanation.  
71 It is really strange that you find zero-valued sensitivities. Also, even if the explanation  
72 holds for snow-related parameters, what about *Drofac*? How is it possible that it has no  
73 influence on RV in any of the catchments? The authors mention that a colleague has  
74 submitted a paper to HESS that strictly examines results of FAST. If more details about  
75 this surprising behavior can be found in that paper, I think it would be good to insert a  
76 reference to that paper here.

77 **Author's response (marked by comments *Bock7* and *Bock8* in this version of**  
78 **manuscript):** We have added a few sentences clarifying what the authors think are the  
79 important aspects of the results shown in Figure 5, and why the *Rfactor* is such an  
80 important parameter to the RV in Region 08 (The Lower Mississippi) as compared to  
81 R14 (Upper Colorado). Our colleague's paper is also still in the review stage at HESS,  
82 and we did not want to cite it at this moment.

83 **Changes in the text:**

84 Section 3.1: Parameter Sensitivities

- 85 ○ Page 11, lines 276-277 – Added the text “and between the RR and RV within a  
86 single region” to emphasize sensitive parameters can vary within a single  
87 geographic locale based on the objective function or model response being  
88 analyzed.

89

90 ○ Page 11, 285-296 – Modified this section as to add some detail to the reviewer’s

91 inquiries about *Drofac* and *Rfactor* above:

92 “In the Lower Mississippi Region the amount of snowfall is negligible, so the

93 three parameters that control snowfall and snowpack accumulation in the MWBM

94 have a negligible effect on the volume and variability of simulated total runoff.

95 The *Rfactor* parameter controls almost all of the model variance for the RV in the

96 Lower Mississippi region. In humid, sub-tropical hydroclimatic regimes of the

97 CONUS, peak runoff is coincident with peak precipitation, which is significant

98 because these periods are when the surplus runoff is greatest. In the Upper

99 Colorado, peak runoff is not coincident with peak precipitation, and the MWBM

100 snow parameters have more control in modulating the variability and timing of

101 runoff in the higher elevation HRUs. The comparison of the parameter

102 sensitivities for these two regions illustrates how variable parameter sensitivities

103 differ by region (i.e. different climatic and physiographic regions) and

104 components of model response (i.e. volume and variability).”

105 **Other Major Changes in the text:**

- 106 • **Comment Bock9 in this version of the manuscript:** The WRR commentary article  
107 “Accelerating advances in continental domain hydrologic modeling” by Archfield et al.  
108 has been published and the citation in the references has been changes to reflect that  
109 information.
- 110 • **Comment Bock10 in this version of the manuscript:** Removed old Figure 3 flow chart  
111 in favor of new one  
112  
113

- 114 • **Comment Bock11 in this version of the manuscript:** Created new Figure 3 flowchart  
115 to better illustrate the Section 3 workflow.
- 116
- 117 • **Comment Bock12 in this version of the manuscript:** Modified Figure 3 caption to  
118 better connect Figure 3 to the Section 3 introductory text
- 119
- 120
- 121
- 122
- 123
- 124
- 125
- 126
- 127
- 128
- 129
- 130
- 131
- 132
- 133
- 134
- 135
- 136
- 137
- 138
- 139
- 140
- 141
- 142
- 143
- 144
- 145
- 146
- 147
- 148
- 149
- 150

151 **Parameter regionalization of a monthly water balance model for**  
152 **the conterminous United States**

153 **A.R. Bock<sup>1</sup>, L.E. Hay<sup>2</sup>, G.J. McCabe<sup>2</sup>, S.L. Markstrom<sup>2</sup>, and R.D. Atkinson<sup>3</sup>**

---

154 <sup>1</sup> U.S. Geological Survey, Colorado Water Science Center, Denver Federal Center, P.O. Box  
155 25046, MS 415, Denver, Colorado, 80225, USA

156 <sup>2</sup> U.S. Geological Survey, National Research Program, Denver Federal Center, P.O. Box 25046,  
157 MS 413, Denver, Colorado, 80225, USA

158 <sup>3</sup> U.S. Environmental Protection Agency, Office of Water (4503-T), 1200 Pennsylvania Ave.,  
159 Washington, DC, 20004, USA

160

161 Correspondence to: A. Bock (abock@usgs.gov)

162

163

164

165

166

167

168

169

170

171

172

173

174

175 **Abstract**

176 A parameter regionalization scheme to transfer parameter values from gaged to ungaged areas  
177 for a monthly water balance model (MWBM) was developed and tested for the conterminous  
178 United States (CONUS). The Fourier Amplitude Sensitivity Test, a global-sensitivity algorithm,  
179 was implemented on a MWBM to generate parameter sensitivities on a set of 109,951 hydrologic  
180 response units (HRUs) across the CONUS. The HRUs were grouped into 110 calibration  
181 regions based on similar parameter sensitivities. Subsequently, measured runoff from 1,575  
182 streamgages within the calibration regions were used to calibrate the MWBM parameters to  
183 produce parameter sets for each calibration region. Measured and simulated runoff at the 1,575  
184 streamgages showed good correspondence for the majority of the CONUS, with a median  
185 computed Nash-Sutcliffe Efficiency coefficient of 0.76 over all streamgages. These methods  
186 maximize the use of available runoff information, resulting in a calibrated CONUS-wide  
187 application of the MWBM suitable for providing estimates of water availability at the HRU  
188 resolution for both gaged and ungaged areas of the CONUS.

189

190

191

192

193

194

195

196

197



198 **Introduction**

199 The WaterSMART program (<http://water.usgs.gov/watercensus/WaterSMART.html>) was started  
200 by the United States (U.S.) Department of the Interior in February 2010. Under WaterSMART,  
201 the National Water Census (NWC) was proposed as one of the U.S. Geological Survey's (USGS)  
202 key research directions with a focus on developing new hydrologic tools and assessments. One  
203 of the major components of the NWC is to provide estimates of water availability at a sub-  
204 watershed resolution nationally (<http://water.usgs.gov/watercensus/streamflow.html>) with the  
205 goal of determining if (1) the Nation has enough freshwater to meet both human and ecological  
206 needs and (2) this water will be available to meet future needs. Streamflow measurements do not  
207 provide direct observations of water availability at every location of interest; approximately 72  
208 percent (%) of land within the conterminous U.S. is gaged, with approximately 13% of these  
209 gaged areas being unaffected by anthropogenic effects (Kiang et al., 2013). This creates the  
210 challenge of determining the best method to transfer information from gaged catchments to data-  
211 poor areas where results cannot be calibrated or evaluated with measured streamflow (Vogel,  
212 2006). This transfer of model parameter information from gaged to ungaged catchments is  
213 known as hydrologic regionalization (Bloschl and Sivapalan, 1995).

214 Many hydrologic regionalization methods have focused on developing measures of similarity  
215 between gaged and ungaged catchments using spatial proximity and physical characteristics.  
216 These methods are highly dependent on the complexity of the terrain and scale at which the  
217 relations are derived. Spatial proximity is considered the primary explanatory variable for  
218 hydrologic similarity (Sawicz et al., 2011) because of the first-order effects of climatic and  
219 topographic controls on hydrologic response. Close proximity, however, does not always result  
220 in hydrologic similarity (Vandewiele and Elias, 1995; Smakhtin, 2001; Ali et al., 2012).

221 Physical characteristics have been used as exploratory variables to develop a better  
222 understanding of the relation between model parameters that represent model function, and  
223 physical properties of the catchment (Merz and Bloschl, 2004). The relation between model  
224 parameters and the relevant physical characteristics, expressed for example as a form of  
225 multivariate regression, can be transferred to ungaged catchments (Merz and Bloschl, 2004).  
226 Model parameter definitions are by nature ambiguous and often difficult to correlate to a small

227 number of meaningful variables such as physical and climatic characteristics (Zhang et al.,  
228 2008); some studies have found no significant correlation between catchment attributes and  
229 model parameters (Seibert, 1999; Peel et al., 2000), whereas others found that high correlation  
230 does not guarantee parameters that result in reliable model simulations of measured data (Sefton  
231 and Howarth, 1998; Kokkonen et al., 2003; Oudin et al., 2010). Physical characteristics also are  
232 used to classify catchments into discrete regions or clusters based on similarity in multi-  
233 dimensional attribute space (Oudin et al, 2008, 2010; Samuel et al., 2011). While these methods  
234 have indicated some success in simulating behavior of specific hydrologic components, such as  
235 base flow (Santhi et al., 2008), other efforts utilizing discrete clusters performed poorly in  
236 explaining variability of measured streamflow (McManamay et al., 2011).

237 Two important components of the transfer of parameters to ungauged catchments are the  
238 identification of (1) influential (and non-influential) parameters, and (2) geographic extents and  
239 scales at which parameters exert control on model function. Reducing the number of parameters  
240 is important for calibration efficiency by reducing the structural bias of the model and the  
241 uncertainty of results where they cannot be verified or confirmed (Van Griensven et al., 2006). A  
242 high number of calibrated, poorly constrained parameters can often mask data or structural  
243 errors, which can go undetected and reduce the skill of the model in replicating results outside of  
244 calibration conditions (Kirchner, 2006; Bloschl et al., 2013). This increases the potential for  
245 equifinality of parameter sets and higher model uncertainty that can be propagated to model  
246 results (Troch et al., 2003).

247 Sensitivity analysis (SA) has advanced the understanding of parameter influence on model  
248 behavior and structural uncertainty. SA measures the response of model output to variability in  
249 model input and/or model parameter values. SA partitions the total variability in the model  
250 response to each individual model parameter (Reusser et al., 2011) and results in a more-defined  
251 set of parameters and parameter ranges. Identification of sensitive parameters and their ranges is  
252 important for hydrologic model applications as key model parameters can vary spatially across  
253 physiographic regions, and also temporally (Tang et al., 2007; Guse et al., 2013).

254 Until recently, the high computational demands of SA have limited most implementations of  
255 hydrologic model SA to local sensitivity algorithms that evaluate a single parameter at a time

256 (Tang et al., 2007). Global SA uses random or systematic sampling designs of the entire  
257 parameter space to quantify variation in model output (Van Griensven et al. 2006, Reusser et al.  
258 2011). Some of these methods can account for parameter interaction and quantify sensitivity in  
259 non-linear systems. Global SA methods are computationally intensive (Cuo et al., 2011), but  
260 ever increasing computational efficiency has allowed for the development and application of a  
261 large number of global SA algorithms.

262 Previous work has suggested that isolating the key parameters that control model performance  
263 can be used to infer dominant physical processes in the catchment, as well as which components  
264 of the model dominate hydrologic response (Van Griensven et al. 2006, Tang et al., 2007,  
265 Reusser et al., 2011). To date, there has been little analysis of the use of SA for deriving  
266 measures of hydrologic similarity across catchments that can be applied towards hydrologic  
267 regionalization of model parameters. The spatially-distributed application of SA could be used  
268 to provide additional information for the delineation of homogeneous regions for parameter  
269 transfer based on similarity of model results from the SA. This strategy allows for the use of the  
270 existing model information and configuration to develop a calibration and regionalization  
271 framework without significantly changing the model structure or implementation

272 In this study, we present a hydrologic regionalization methodology for the CONUS that derived  
273 regions of hydrologic similarity based on the response of a Monthly Water Balance Model  
274 (MWBM) to parameter SA. Groups of streamgages within each region are calibrated together to  
275 define a single parameter set for each region. By extending model calibration to a large number  
276 of sites grouped by similarity through a quantified measure of model behavior, a more specific  
277 and constrained parameter space that fits each region can be identified.

## 278 **Methods**

### 279 **2.1 Monthly Water Balance Model**

280 The MWBM (Fig. 1) is a modular accounting system that provides monthly estimates of  
281 components of the hydrologic cycle by using concepts of water supply and demand (Wolock and  
282 McCabe 1999; McCabe and Markstrom, 2007). Monthly temperature (T) is used to compute  
283 potential evapotranspiration (PET) and to partition monthly precipitation (P) into rain and snow

284 (Fig. 1). Precipitation that occurs as snow is accumulated in a snow pack (snow storage as snow  
285 water equivalent, or SWE); rainfall is used to compute direct runoff ( $R_{\text{direct}}$ ) or overland flow,  
286 actual evapotranspiration (AET), soil-moisture storage recharge, and surplus water, which  
287 eventually becomes runoff (R) (Fig. 1). When rainfall for a month is less than PET, AET is equal  
288 to the sum of rainfall, snowmelt, and the amount of moisture that can be removed from the soil.  
289 The fraction of soil-moisture storage that can be removed as AET decreases linearly with  
290 decreasing soil-moisture storage; that is, water becomes more difficult to remove from the soil as  
291 the soil becomes drier and less moisture is available for AET. When rainfall (and snowmelt)  
292 exceeds PET in a given month, AET is equal to PET; water in excess of PET replenishes soil-  
293 moisture storage. When soil-moisture storage reaches capacity during a given month, the excess  
294 water becomes surplus and a fraction of the surplus ( $R_{\text{surplus}}$ ) becomes R, while the remainder of  
295 the surplus is temporarily held in storage. The MWBM has been previously used to examine  
296 variability in runoff over the CONUS (Wolock and McCabe, 1999; Hay and McCabe 2002;  
297 McCabe and Wolock, 2011a) and the global extent (McCabe and Wolock, 2011b). Table 1 lists  
298 the MWBM parameters, with definitions and parameter ranges for calibration.

299 The *Ppt\_adj* and *Tav\_adj* parameters specify seasonal adjustments for precipitation and  
300 temperature, respectively. The seasonal adjustment parameters were included to account for  
301 errors in the precipitation and temperature data used in this analysis. Sources of systematic and  
302 non-systematic errors of climate forcing data are well documented from the precipitation gage-  
303 derived sources (Groisman and Legates, 1994; Adam and Lettenmaier, 2003). Interpolation of  
304 these systematic errors from point-scale to gridded domains may propagate these biases,  
305 especially in complex terrain (Clark and Slater, 2006; Oyler et al, 2015). The use of adjustment  
306 factors allows uncertainty associated with forcing data and model parameter values to be treated  
307 separately (Vrugt et al., 2008).

308 *Figure 1. Conceptual diagram of the Monthly Water Balance Model (McCabe and Markstrom*  
309 *2007). Processes influenced by model parameters used in Fourier Amplitude Sensitivity Test*  
310 *(FAST) those identified by green arrow and numbered 1-5 (Table 1).*

311 [Monthly Water Balance Model parameters and ranges.](#)

312 The MWBM was applied to the CONUS with 109,951 hydrologic response units (HRUs) from  
313 the Geospatial Fabric (Viger and Bock, 2014), a national database of hydrologic features for  
314 national hydrologic modeling applications (Fig. 2). This HRU derivation is based on an  
315 aggregation of the NHDPlus dataset (<http://www.horizon-systems.com/nhdplus/>), an integrated  
316 suite of geospatial data that incorporates features from the National Hydrography Dataset  
317 (<http://nhd.usgs.gov/>), the National Elevation Dataset (<http://ned.usgs.gov/>), and the Watershed  
318 Boundary Dataset (<http://nhd.usgs.gov/wbd.html>). The sizes of the HRUs range from less than 1  
319 square kilometer (km<sup>2</sup>) up to 67,991 km<sup>2</sup>, with an average size of 74 km<sup>2</sup>.

320 Inputs to the MWBM by HRU are: (1) monthly P (millimeters), monthly mean T (degrees  
321 Celsius), (2) latitude of the site (decimal degrees), (3) soil moisture storage capacity  
322 (millimeters), and (4) monthly coefficients for the computation of PET (dimensionless).  
323 Monthly P and mean T were derived from the daily time step, 1/8° gridded meteorological data  
324 for the period of record from January 1949 through December 2011 (Maurer et al., 2002).  
325 Monthly P and T data were aggregated for each HRU using the USGS Geo Data Portal  
326 (<http://cida.usgs.gov/climate/gdp/>) (Blodgett et al., 2011). Latitude was computed from the  
327 centroid of each HRU. Soil moisture storage capacity was calculated using a 1 km<sup>2</sup> grid derived  
328 from the Soils Data for the Conterminous United States (STATSGO) (Wolock, 1997). The  
329 monthly PET coefficients were calculated by calibrating the Hamon PET values to Farnsworth et  
330 al. (1982) mean monthly free-water surface evapotranspiration. McCabe et al. (2015) describes  
331 these PET coefficient calculations in detail.

332 *Figure 2. Hydrologic Response Units of the Geospatial Fabric, differentiated by color, overlain*  
333 *by NHDPlus region boundaries (R01-R18).*

## 334 **2.2 Fourier Amplitude Sensitivity Test**

335 A parameter SA for the CONUS was conducted for the MWBM using the Fourier Amplitude  
336 Sensitivity Test (FAST) to identify areas of hydrologic similarity. FAST is a variance-based  
337 global sensitivity algorithm that estimates the contribution to model output variance explained by  
338 each parameter (Cukier et al. 1973, 1975; Saltelli et al. 2000). Advantages of using FAST over  
339 other SA methods are that FAST can calculate sensitivities in non-linear systems, and is

340 extremely computationally efficient. The seasonal adjustment factors were not incorporated into  
341 the FAST analysis. We viewed the seasonal adjustment factors as more related to the forcing  
342 data, and for this application only parameters associated with model structure were included  
343 (first five parameters in Table 1).

344 FAST transforms a model's multi-dimensional parameter space into a single dimension of  
345 mutually independent sine waves with varying frequencies for each parameter, while using the  
346 parameter ranges to define each wave's amplitude (Cuker et al. 1973, 1975; Reusser et al. 2011).  
347 This methodology creates an ensemble of parameter sets numbering from 1 to N, each of which  
348 is unique and non-correlated with the other sets. Parameter sets are derived using the  
349 corresponding y-values along each parameter's sine wave given a value on the x-axis. The  
350 model is executed for all parameter sets using identical climatic and geographic inputs for each  
351 simulation. The resulting series of model outputs are Fourier-transformed to a power spectrum  
352 of frequencies for each parameter. Parameter sensitivity is calculated as the sum of the powers  
353 of the output variance for each parameter, divided by the sum of the powers of all parameters  
354 (Total Variance). The parameter sensitivities are scaled so that the sensitivities for all  
355 parameters sum to 1. Thus, parameters that explain a large amount of variability in the model  
356 output have higher (i.e. closer to 1) parameter sensitivity values.

357 FAST was implemented with the MWBM using the 'fast' library in the statistical software R  
358 (Reusser, 2012; R Core Team, 2013). Parameter ranges used by FAST for generating wave  
359 amplitudes of parameter ensembles across the CONUS were based on table 1. The 'fast' R  
360 package pre-determines the minimal number of runs necessary to estimate the sensitivities for  
361 the given number of parameters (Cukier et al., 1973). For our application we generated an  
362 ensemble of 1000 parameter sets (as compared to the minimally suggested number of 71  
363 estimated by 'fast'). The use of the minimal number of parameter sets should be a consideration  
364 for more complex models, but the relative computational efficiency and parallelization of the  
365 MWBM allowed the model to be simulated with this larger number of parameter sets quickly to  
366 help ensure a robust parameter sensitivity analysis.

367 Many applications of SA in hydrologic modeling have evaluated parameter sensitivity for  
368 measured streamflow using performance-based measures such as bias, root mean squared error

**Comment [Bock1]:** Reviewer comment #1:  
Unclear, it seems to me that no other SA  
method was applied. The only reason I see  
here to increase the sample size is to increase  
the robustness of the sensitivity estimates  
produced by FAST.

**Comment [Bock2]:** Modifications to text in  
response to reviewer comment #1

369 (RMSE), and the Nash-Sutcliffe Efficiency (NSE) (Nash and Sutcliffe, 1970; Moriasi et al.,  
370 2007). In this study, parameter sensitivity is examined using two hydroclimatic indices that  
371 account for the magnitude and variability of both climatic input and model output: the (1) Runoff  
372 Ratio (RR), a ratio of simulated runoff to precipitation, and (2) Runoff Variability (RV) index,  
373 the standard deviation of simulated runoff to the standard deviation of precipitation  
374 (Sankarasubramanian and Vogel, 2003).

### 375 **Parameter regionalization procedure**

376 The following sections describe the workflow for the MWBM calibration and regionalization  
377 (illustrated in Figure 3). The MWBM parameter sensitivities from the FAST analysis were  
378 evaluated across the CONUS. The spatial patterns and magnitudes of parameter sensitivities  
379 were used to organize the 109,951 HRUs into hydrologically similar regions referred to in the  
380 paper as calibration regions. During the initial streamgauge selection, potential streamgages were  
381 identified for use in the grouped MWBM calibration. These selected streamgages then were  
382 individually calibrated. Using a number of selection criteria, a final set of calibration gages were  
383 derived within each calibration region. The grouped MWBM calibration produced an ‘optimal’  
384 set of MWBM parameters for each calibration region by evaluating simulated MWBM variables  
385 converted to Z-scores.

386 *Figure 3. Schematic flowchart of the parameter regionalization procedure described in Section*  
387 *3: Parameter sensitivities (3.1), Calibration regions (3.2), Initial streamgauge selection (3.3),*  
388 *and Grouped streamgauge calibration (3.4).*

### 389 **3.1 Parameter sensitivities**

390 The relative sensitivities derived from the FAST analysis using the RR and RV indices at each of  
391 the 109,951 HRUs across the CONUS were scaled so that the five MWBM parameter  
392 sensitivities derived for each HRU summed to 100 (Fig. 4). RR (Fig. 4a) is most sensitive to the  
393 parameter *Drofac* in regions where MWBM runoff is not dominated by snowmelt and orographic  
394 precipitation, such as arid and sub-tropical areas of the CONUS. MWBM parameters that  
395 control snowpack accumulation and melt (*Meltcoef*, *Tsnow*, and *Train*) are more important to the  
396 RR in the extensive mountain ranges in the Western CONUS, and northerly latitudes around the

**Comment [Bock3]:** Reviewer Comment #2:  
Maybe worth inserting a short explanation of the  
key steps of the procedure? The figure is helpful  
but not self-explaining

**Comment [Bock4]:** AB response: I re-  
designed the flow chart and the wording of this  
first paragraph to more easily guide readers  
through the workflow of Section 3. I've also  
modified the Figure 3 caption.

**Comment [Bock5]:** Modified caption for figure  
3 to add more description

397 Great Lakes and in the Eastern CONUS. The RR indicates the highest sensitivity to the *Rfactor*  
398 parameter in mountainous areas of the CONUS and areas of the West Coast, and moderate to  
399 high sensitivity in areas where the sensitivity of RR to *Drofac* is low. *Tsnow*, *Train*, and  
400 *Meltcoef* all share similar patterns across the CONUS. The spatial variability of the sensitivity of  
401 RR to *Meltcoef* indicates different physical mechanisms controlling *Meltcoef* parameter influence  
402 on RR in different areas of the CONUS. In the Western CONUS, the sensitivity of RR to  
403 *Meltcoef* is greatest in mountainous areas that accumulate and hold snowpack through the late  
404 spring, such as the Rocky Mountains, Cascade, and Sierra Nevada mountain ranges. In the  
405 Eastern and Midwestern CONUS, the sensitivity of RR to *Meltcoef* is greatest for HRUs with  
406 more northerly latitudes.

407 *Figure 4. Relative sensitivity of the (a) Rainfall Ratio (RR) and (b) Runoff Variability (RV)*  
408 *indices to Monthly Water Balance Model parameters.*

409 The spatial patterns of sensitivities of RV to the five MWBM parameters (Fig. 4b) show both  
410 similarities and deviations from the patterns shown in the RR maps. For the central part of the  
411 CONUS, the relative sensitivity for the parameter *Drofac* is high for both indices, and low for the  
412 parameter *Rfactor* for both indices. *Meltcoef*, *Tsnow*, and *Train* share the same relations between  
413 higher sensitivity and higher elevation (primarily in the western part of the CONUS), and higher  
414 sensitivity and more northerly latitude (primarily in the eastern half of the CONUS) for both  
415 indices. However, *Drofac* and *Rfactor* show distinctly different patterns of relative sensitivities  
416 for the eastern part of the CONUS for RV as compared to RR. The other three parameters  
417 follow the same general spatial patterns for RV as compared to RR, but with greater fine-scale  
418 spatial variation and patchiness. The differences between the spatial distributions of the  
419 sensitivities between the two indices highlight that applying SA to different model outputs can  
420 generate different levels of sensitivities for each parameter. In addition, the choice of objective  
421 function or model output for which to measure parameter sensitivity is important, as parameter  
422 sensitivities will differ depending on whether a user evaluating measures of magnitude, the  
423 variability of distribution, or timing (Krause et al., 2005; Kapangaziwiri et al, 2012).

424 [Figure 5](#) illustrates the variability of parameter sensitivities between NHDPlus regions 08 (Lower  
425 Mississippi) and 14 (Upper Colorado) (see Fig. 2) for the RR and RV indices, and between the

**Comment [Bock6]:** Reviewer comment #3: I am still not persuaded by this explanation. It is really strange that you find zero-valued sensitivities. Also, even if the explanation holds for snow-related parameters, what about *Drofac*? How is it possible that it has no influence on RV in any of the catchments? The authors mention that a colleague has submitted a paper to HESS that strictly examines results of FAST. If more details about his surprising behavior can be found in that paper, I think it would be good to insert a reference to the paper here.

**Comment [Bock7]:** AB response: I added more details on our interpretations of the SA results on the bottom part of the paragraph (as well as modified some text in a few places to add more detail)



426 RR and RV within a single region. The Lower Mississippi and Upper Colorado NHDPlus  
427 regions have a similar number of HRUs (4,449 and 3,879, respectively) and cover a similar area  
428 (26,285 and 29,357 km<sup>2</sup>, respectively). The Lower Mississippi region has homogenous  
429 topography, with humid, subtropical climate, while the Upper Colorado region has highly  
430 variable topography, and thus highly variable climatic controls on hydrologic processes. For the  
431 Lower Mississippi region only one parameter dominates modeled RV variance (*Rfactor*, Fig. 5a)  
432 and modeled RR variance (*Drofac*, Fig. 5c). In contrast, for the Upper Colorado River region  
433 several parameters influence RV variability (*Drofac*, *Rfactor* and *Meltcoef*, Fig. 5b) and RR  
434 variability (*Drofac* and *Meltcoef*, Fig. 5d). In the Lower Mississippi Region the amount of  
435 snowfall is negligible, so the three parameters that control snowfall and snowpack accumulation  
436 in the MWBM have a negligible effect on the volume and variability of simulated total runoff.  
437 The *Rfactor* parameter controls almost all of the model variance for the RV in the Lower  
438 Mississippi region. In humid, sub-tropical hydroclimatic regimes of the CONUS, peak runoff is  
439 coincident with peak precipitation, which is significant because these periods are when the  
440 surplus runoff is greatest. In the Upper Colorado, peak runoff is not coincident with peak  
441 precipitation, and the MWBM snow parameters have more control in modulating the variability  
442 and timing of runoff in the higher elevation HRUs. The comparison of the parameter  
443 sensitivities for these two regions illustrates how variable parameter sensitivities differ by region  
444 (i.e. different climatic and physiographic regions) and components of model response (i.e.  
445 volume and variability).

Comment [Bock8]: Additions to the text for reviewer comment #3

446 *Figure 5. Parameter sensitivities of Runoff Variability (RV; a-b) and Runoff Ratio (RR; c-d)*  
447 *indices for Monthly Water Balance Model parameters in the Lower Mississippi (R08) and*  
448 *Upper Colorado (R14).*

### 449 3.2. Calibration regions

450 The spatial patterns and magnitudes of parameter sensitivities across the CONUS were used as a  
451 basis for organizing HRUs into hydrologically similar regions for parameter regionalization  
452 through MWBM calibration. This idea is rooted in the hypothesis that geographically proximate  
453 HRUs share similar forcings and conditions, and thus will behave similarly. This application  
454 uses similarity in SA results as a basis for organization, rather than similarity in physiographic

455 characteristics. The derived regions are subsequently used to simplify model calibration across  
456 the CONUS and provide a basis for the transfer and application of parameters to ungauged areas.

457 The parameter sensitivities derived from the RR were used to organize the HRUs into two  
458 independently-derived calibration regions; the first derived by identifying HRUs with unique  
459 combinations of the order of parameter sensitivities to the RR (highest parameter sensitivities to  
460 lowest, i.e. 1-*Drofac* (78%), 2-*Rfactor* (16%), 3-*Meltcoef* (5%), 4-*Tsnow* (1%), 5-*Train* (1%)),  
461 and the second classification based upon identifying HRUs with unique sets of parameters whose  
462 sensitivities exceeded a specified threshold of parameter sensitivity (i.e. only *Drofac*, *Rfactor*,  
463 *Meltcoef* using a 5% threshold in the first classification example). The purpose of the first  
464 classification was to delineate regions of similar model response or behavior based on the order  
465 of importance of the MWBM parameters to the RR for each HRU. This classification identified  
466 16 distinct regions of HRUS across the CONUS based on the order of the parameter sensitivities  
467 of the five parameters (derived using the RR index). Sizes of these regions ranged from 94 km<sup>2</sup>  
468 to almost 2 million km<sup>2</sup>. The second classification delineated regions with an identical set of the  
469 most important parameters to the RR based on parameters whose sensitivities exceeded a 5%  
470 threshold. This step identified 12 regions of HRUs with unique combinations of parameter  
471 sensitivities exceeding 5%. There has been progress in providing quantitative thresholds for the  
472 identification of sensitive and non-sensitive parameters for hydrologic modelers (Tang et al.,  
473 2007), but no definitive consensus yet exists. Therefore a 5% threshold was used based on visual  
474 delineation of major physiographic features such as mountain ranges across the CONUS. The  
475 sizes of this second group of regions ranged from 94 km<sup>2</sup> to more than 15 million km<sup>2</sup>. Maps of  
476 the two groupings of HRUS were intersected to create a total of 49 regions across the CONUS.  
477 NHDPlus region and sub-region boundaries, proximity, and significant topographic divides were  
478 used to further divide the groups into 159 geographically unique calibration regions across the  
479 CONUS. The lack of streamgages available in some regions, especially areas with arid and  
480 semi-arid climates, necessitated merging regions together. Calibration regions that contained  
481 less than 3 streamgages from the 8,410 gages present in the Geospatial Fabric (see section 3.3)  
482 were combined with the proximate and most similar group which shared the most similar  
483 parameter sensitivities (both order and magnitude), resulting in 110 calibration regions across  
484 the CONUS (Fig. 6). Within each region the FAST results for both the RR and RV indices were

485 used to determine which parameters to calibrate. Within each region, parameters with a median  
486 parameter sensitivity of 5% for the RR and RV among the region's HRUs were selected for  
487 group calibration. Parameters not shown as sensitive were kept at the default value for the  
488 group.

489 *Figure 6. Final 110 Monthly Water Balance Model calibration regions differentiated by colors.*  
490 *A subset of streamgages within each calibration region were calibrated in a group-wise*  
491 *fashion to produce a single optimized parameter set for the entire region (Fig. 3).*

### 492 **3.3 Initial streamgage selection**

493 The initial set of streamgages used for testing in the MWBM calibration procedures was selected  
494 from 8,410 streamgages identified in the Geospatial Fabric (Fig. 7). The Geospatial Fabric  
495 includes reference and non-reference streamgages from the Geospatial Attributes of Gages for  
496 Evaluating Streamflow dataset (GAGES-II, Falcone et al., 2010). Of the 8,410 streamgages in  
497 the Geospatial Fabric, 1,864 were identified as having reference-quality data with at least 20  
498 years of record. These reference quality streamgages were judged to be largely free of human  
499 alterations to flow (Falcone et al., 2010). In the current study, reference quality was not  
500 considered in the initial streamgage selection because the 20 years of record was considered too  
501 restrictive. Therefore a subset of the 8,410 streamgages was selected for initial testing in the  
502 MWBM calibration procedures based on the following criteria:

- 503 (1) Remove streamgages with less than 10 years of total measured streamflow (120 months)  
504 within the time period 1950 – 2010.
- 505 (2) Remove streamgages with a drainage area defined by the Geospatial Fabric that are not  
506 within 5% of the USGS National Water Information System (NWIS) reported drainage  
507 area (U.S. Geological Survey, 2014). This eliminated many of the streamgages with  
508 smaller drainage areas due to the resolution of the Geospatial Fabric.
- 509 (3) Remove streamgages that did not have at least 75% of its drainage area contained within  
510 a single calibration region.

511 These criteria resulted in 5,457 potential streamgages for testing in the MWBM calibration  
512 procedures (Fig. 7). Streamflow at these streamgages was aggregated and converted from daily  
513 (cubic feet/second) to a monthly runoff depth (mm) (streamflow per unit area).

514 *Figure 7. Streamgages tested in the study. GF notes geospatial fabric for national hydrologic*  
515 *modeling (Viger and Bock, 2014).*

### 516 **3.4 Monthly Water Balance Model calibration**

517 Two automated calibration procedures were implemented to produce an ‘optimal’ set of MWBM  
518 parameters for each calibration region. The first procedure, Individual Streamgage Calibration,  
519 calibrated each of the 5,457 streamgages individually. Results from the individual calibrations  
520 were used to further filter the streamgages within the second procedure, Grouped Streamgage  
521 Calibration, which calibrated selected streamgages together by calibration region.

#### 522 **3.4.1 Individual streamgage calibration**

523 The first calibration procedure was an automated process that individually calibrated each of the  
524 5,457 streamgages from the initial streamgage selection with measured streamflow (U.S.  
525 Geological Survey, 2014). Results from these individual streamgage calibrations quantified the  
526 ‘best’ performance of the MWBM at each gage, providing a ‘baseline’ measure for evaluation.

527 The Shuffled Complex Evolution (SCE) global-search optimization algorithm (Duan et al., 1993)  
528 has been frequently used as an optimization algorithm in hydrologic studies (Hay et al., 2006;  
529 Blasone et al. 2007; Arnold et al., 2012), including previous studies with the MWBM (Hay and  
530 McCabe, 2010). Further details can be found in Duan et al. (1993). SCE was used to maximize a  
531 combined objective function based on: (1) Nash-Sutcliffe Efficiency (NSE) coefficient using  
532 measured and simulated monthly runoff and (2) NSE using natural log-transformed measured  
533 and simulated runoff (logNSE), using the entire period of record for each streamgage. The NSE  
534 measures the predictive power of the MWBM in matching the magnitude and variability of the  
535 measured and simulated runoff (Nash and Sutcliffe, 1970). The NSE coefficient ranges from  $-\infty$   
536 to 1, with 1 indicating a perfect fit, and values less than 0 indicating that measured mean runoff  
537 is a better predictor than model simulations. The NSE has been shown to give more weight to  
538 the larger values in a time series (peak flows) at the expense of lower values (low flows)

539 (Legates and McCabe, 1999), so the logNSE was incorporated into the objective function to give  
540 weight to lowflow periods (Tekleab et al., 2011).

### 541 **3.4.2 Grouped streamgage calibration**

542 The second calibration procedure was an automated process that calibrated groups of  
543 streamgages together for each calibration region to derive a single set of MWBM parameters  
544 (Table 1) for each calibration region (Fig. 6). The NSE and logNSE values from the individual  
545 streamgage calibrations (described in the previous section) were used to identify streamgages  
546 that should not be used for grouped streamgage calibration. If the individual streamgage  
547 calibration was not ‘satisfactory’, then it was felt that it would not provide useful information for  
548 the grouped streamgage calibration procedure.

549 Satisfactory individual streamgage calibrations were identified with the following procedure:

- 550 (1) Eliminate all streamgages with NSE values  $< 0.3$ .
- 551 (2) If the number of remaining streamgages for a given calibration region is  $> 10$ , then  
552 eliminate all streamgages with NSE  $< 0.5$ .
- 553 (3) If the number of streamgages for a given calibration region is  $> 25$ , then eliminate all  
554 streamgages with  $NSE_{log} < 0$ .
- 555 (4) If the number of remaining streamgages for a calibration region is  $< 5$ , check to see if any  
556 of the eliminated streamgages were reference streamgages (as defined in Falcone et al, 2010),  
557 then add the reference streamgages back in if the NSE value  $> 0.0$ . Reference streamgages are  
558 USGS streamgages deemed to be largely free of anthropogenic impacts and flow modifications  
559 (Falcone et al., 2010; Kiang et al., 2013).

560 These criteria, while somewhat arbitrary, were chosen so that no calibration region had less than  
561 5 streamgages for the grouped streamgage calibration. Using the above criterion, of the 5,457  
562 streamgages individually calibrated, 3,125 remained as candidates for the grouped streamgage  
563 calibration procedure.

564 The grouped streamgauge calibration procedure used the SCE global-search optimization  
 565 algorithm with a multi-term objective function (Eq. 1). Measured and simulated values for  
 566 selected streamgages contained within a calibration region were scaled to Z-scores to remove  
 567 differences in magnitudes between streamgages (Eq. 2). The multi-term objective function  
 568 minimized the sum of the absolute differences between Z-scores from four measured and  
 569 simulated time series: mean monthly runoff (MMO, MMS), monthly runoff (MO, MS), annual  
 570 runoff (AO, AS) (U.S. Geological Survey, 2014), and monthly snow water equivalent (SO, SS))  
 571 for all selected streamgages within a given calibration region:

$$572 \quad \min \sum_{i=1}^n [3|MMO_i - MMS_i| + |MO_i - MS_i| + |AO_i - AS_i| + 0.5|SO_i - SS_i|] \quad (\text{Eq.1})$$

573

$$\text{where } \begin{cases} 0 & \text{if } 0.75 < SO_i - SS_i < 1.25 \\ |SO_i - SS_i| & \text{if } SS_i < SO_i^{0.75} \\ |SO_i - SS_i| & SS_i > SO_i^{1.25} \end{cases}$$

574 The measured and simulated Z-scores were calculated as:

$$575 \quad Z = (x-u)/\sigma \quad (\text{Eq. 2})$$

576 where x is the time-series value, u is the mean, and  $\sigma$  the standard deviation of the measured and  
 577 simulated variable.

578 ‘Measured’ SWE was determined for each HRU from the Snow Data Assimilation System  
 579 (SNODAS; National Operational Hydrologic Remote Sensing Center, 2004) and included a +/-  
 580 25% error bound. The unconstrained automated calibration (without a restriction on SWE) led to  
 581 unrealistic sources of snowmelt in the summer that enhanced the low-flow simulations. The 25%  
 582 error bound is arbitrary; calibrating to the actual SNODAS SWE values was found to be too  
 583 restrictive, but adding this error bound to the SWE values resulted in better overall runoff  
 584 simulations. The absolute difference of the simulated SWE Z-scores that were within +/- 25% of  
 585 the measured SWE Z-score were designated as 0. Otherwise, the absolute difference was  
 586 computed between the simulated SWE Z-score and either the upper or lower bounds (Eq. 1).

577 The grouped calibration procedure was run for all 110 calibration regions. For each calibration  
 578 region the seasonal adjustment parameters and the sensitive parameters (identified by the FAST

589 analysis -- section 3.1) were calibrated; parameters deemed not sensitive (parameter sensitivity <  
590 5% of total variance) were set to their default values (see Table 1). The entire period of the  
591 streamflow record for each streamgage was split by alternating years. After calibration, mean  
592 monthly measured and simulated Z-scores for runoff at all selected streamgages within a  
593 calibration region were compared.

594 Figure 8 shows an example of the graphic used to evaluate the measured and simulated mean  
595 monthly Z-scores for 21 streamgages selected for the region located in the Tennessee River  
596 calibration region (part of NHDPlus Region R06 in Fig. 2); the orange, red, and black dots  
597 indicate calibration, evaluation, and the entire period of record, respectively. A tight grouping  
598 around the one-to-one line indicates good correspondence between measured and simulated Z-  
599 scores. Points closer to the upper right corner of each plot represent high-flow periods. Points  
600 closer to the lower left corner of the plot represent low-flow periods. Streamgages within a  
601 calibration region were assigned the same parameter values; therefore streamgages that plotted  
602 outside (two standard deviations) of the one-to-one line were considered to not be representative  
603 of the calibration region, and the calibration procedure for that calibration region was repeated  
604 without those streamgages.

605 *Figure 8. Measured versus simulated mean monthly Z-scores for the Tennessee River*  
606 *calibration region (see Fig. 10b for location). Orange is calibration, red is evaluation, and*  
607 *black is all years.*

608 The goal of the second calibration procedure was to find a single parameter set for each  
609 calibration region. Past applications of the MWBM (Wolock and McCabe, 1999, McCabe and  
610 Wolock, 2011a) used a single set of fixed MWBM parameters for the entire CONUS. Many of  
611 the streamgages included in the second calibration procedure could be affected by significant  
612 anthropogenic effects; the seasonal adjustment factors, calibrated at each individual streamgage,  
613 could account for these effects and result in satisfactory NSE values. Streamgages that were  
614 removed due to poor performance in the second calibration were assumed to have anthropogenic  
615 effects not consistent with the streamgages that plotted along the one-to-one line. Poor  
616 performance may result because the MWBM fails to reliably simulate runoff for a watershed  
617 because of model limitations (i.e. not including all important hydrologic processes), but the

618 calibration regions are assumed to be homogeneous based on the FAST analysis. Therefore it is  
619 assumed that if some of the streamgages within a region have satisfactory results, then the  
620 MWBM is able to simulate runoff in that region.

## 621 **MWBM calibration region results**

### 622 **4.1 Individual streamgage calibration results**

623 The individual streamgage calibrations provided information regarding: (1) the potential  
624 suitability of a given streamgage for inclusion in a grouped calibration, and (2) a ‘baseline’  
625 measure for evaluation of the grouped calibration results. Reference and non-reference  
626 streamgages were considered in this application; if the runoff at a streamgage could not be  
627 calibrated individually to a ‘satisfactory’ level (based on criterion outlined in section 3.4.2), then  
628 it was felt that it would not provide useful information for the grouped streamgage calibration  
629 procedure. Figure 9 shows the NSE (Fig. 9a) and logNSE (Fig. 9b) coefficients from the  
630 individual streamgage calibrations for the CONUS. Scattered throughout the CONUS are NSE  
631 and logNSE values less than 0.0 (triangles in Fig. 9). These poor results are likely streamgages  
632 with poor streamflow records, either due to measurement error or anthropogenic effects (dams,  
633 water use, etc.).

634 *Figure 9. Individual streamgage calibration results: (a) Nash-Sutcliffe Efficiency (NSE)*  
635 *coefficient and (b) log of the NSE (logNSE).*

### 636 **4.2 Grouped streamgage calibration results**

#### 637 **4.2.1 Mean monthly z-scores**

638 Figure 10a shows a scatterplot of measured versus simulated mean monthly Z-scores for runoff,  
639 similar to Figure 8, but based on all available years (the black dots in Fig. 8) for all the final  
640 calibration streamgages (1,575 streamgages). Four regions are highlighted to illustrate the  
641 monthly variability in MWBM results across the CONUS (see Fig. 10b for locations). The four  
642 regions are: New England (67 streamgages, red); Tennessee River basin (21 streamgages,  
643 orange); Platte Headwaters (15 streamgages, blue); and Pacific Northwest (33 streamgages,  
644 green) (Fig. 10b).



645 *Figure 10. (a) Measured versus simulated mean monthly Z-scores for runoff at all streamgages*  
646 *and (b) location of highlighted streamgages for four calibration regions: New England (67*  
647 *streamgages, red); Tennessee River (21 streamgages, orange); Platte Headwaters (15*  
648 *streamgages, blue); and Pacific Northwest (33 streamgages, green).*

649 In Fig. 10a, three of the regions (New England, Tennessee River, and Pacific Northwest), show  
650 simulated Z-scores that correspond favorably to measured Z-scores for each of the twelve  
651 months, including periods of low and high runoff. These regions represent marine or humid  
652 climates with homogenous physio-climatic conditions and an even spatial distribution of  
653 streamgages, where models should be expected to perform well (see Fig. 9) There is a higher  
654 variability in model results for the high-flow months (May - June) for streamgages within the  
655 Platte Headwaters (Fig. 10a; blue dots) than for low-flow months. This variability may be  
656 related to factors controlling the magnitude and timing of snow melt runoff (Fig. 9).

657 For each calibration streamgage, a set of four months were identified that represent different  
658 parts of the measured mean monthly hydrograph (highest- and lowest- flow month and the two  
659 median-flow months). The measured and simulated mean monthly streamflow Z scores  
660 corresponding to the four months are plotted as cumulative frequencies (Fig. 11) to compare how  
661 well the simulated Z scores matched measured Z scores for different parts of the hydrograph  
662 over the entire set of calibration gages. For the highest-flow, there is an under-estimation of  
663 runoff, with the greatest divergence between the two distributions in the middle to lower half of  
664 the distribution (Fig. 11a). For the median-flow, the measured and simulated Z scores are well  
665 matched. For the 10 lowest-flow, simulated Z scores are greater than measured Z scores, with the  
666 greatest divergence between the two distributions in the middle to upper half of the distribution  
667 (Fig. 11c).

668 *Figure 11. Z-score cumulative frequency for (a) highest-, (b) median-, and (c) lowest-flow*  
669 *months.*

670 The median Z-score errors (simulated - measured) by region for the (a) highest-, (b) median-,  
671 and (c) lowest-flows are shown in Figure 12. The largest errors are for the highest-flows (Fig.  
672 12a). The MWBM simulations under-estimate the highest flows for much of the CONUS. The

673 errors for median-flows are fairly uniform and consistent across the CONUS (Fig. 12b), with a  
674 median error close to 0. For the lowest-flow months the MWBM over-estimates low flows for a  
675 large portion of the Midwest (Fig. 12c).

676 *Figure 12. Z-score error (simulated - measured) for (a) highest-, (b) median-, and (c) lowest-*  
677 *flow months.*

#### 678 **4.2.2 Nash-Sutcliffe efficiency**

679 Figure 13 compares the NSE from the individual streamgage calibrations (gageNSE) with the  
680 grouped calibrations (groupNSE) for all final streamgages used in the second calibration  
681 procedure. NSE values  $> 0.75$  (dashed line) and  $> 0.5$  (solid line) indicate very good and  
682 satisfactory results (Moriassi et al., 2007). Overall, most NSE values fall above the 0.5 NSE  
683 threshold of satisfactory performance (median of gageNSE and groupNSE = 0.76). The gageNSE  
684 values are used here as a ‘baseline’ for evaluation of the groupNSE results. The groupNSE  
685 values were not expected to be greater than the gageNSE values since (1) NSE was not used as  
686 an objective function in the grouped calibration, and (2) grouped calibrations found the ‘best’  
687 parameter set for a set of streamgages versus an individual streamgage. Figure 13 shows an equal  
688 distribution of NSE values around the one-to-one line, indicating that the grouped calibration  
689 provided additional information over the individual streamgage calibrations (cases where  
690 groupNSE are greater than gageNSE in Fig. 13). The difference between the gageNSE and  
691 groupNSE becomes larger as the NSE values decrease, reflecting the increasing uncertainty in  
692 the grouped calibrations in areas with lower gageNSE values.

693 *Figure 13. Nash Sutcliffe Efficiency from individual (gageNSE) and grouped (groupNSE)*  
694 *calibration. Calibration regions in New England (67 streamgages, red); Tennessee River*  
695 *(21 streamgages, orange); Platte Headwaters (15 streamgages, blue); and Pacific Northwest*  
696 *(33 streamgages, green) are highlighted (see Fig. 10b for location).*

697 Four regions are highlighted in Fig. 13 to illustrate the variability of NSE across the CONUS  
698 (see Fig. 10b for locations). The highlighted regions in New England (red), Tennessee River  
699 (orange), and Pacific Northwest (green), show good groupNSE and gageNSE results. Four of

700 the 15 streamgages in the Platte Headwaters (blue) have groupNSE values  $\leq 0.5$ . This is  
701 probably related to simulation error during the snowmelt period (May - June, Fig. 10a).

702 Figure 14 shows the median groupNSE by calibration region for the CONUS. The pattern is very  
703 similar to that shown for the individual streamgage calibration results in Fig. 9a and highlights  
704 the problem areas shown in Fig. 12.

705 *Figure 14. Median Nash Sutcliffe Efficiency (NSE) of streamgages used for calibration by*  
706 *calibration region.*

707

## 708 **Discussion**

709 This study presented a parameter regionalization procedure for calibration of the MWBM,  
710 resulting in an application that can be used for simulation of hydrologic variables for both gaged  
711 and ungaged areas in the CONUS. The regionalization procedure grouped HRUs on the basis of  
712 similar sensitivity to five model parameters. Parameter values and model uncertainty  
713 information within a group was then passed from gaged to ungaged areas within that group.

### 714 **5.1 Regionalized parameters**

715 Results from this study indicate that regionalized parameters can be used to produce satisfactory  
716 MWBM simulations in most parts of the CONUS (Fig. 13). Despite the differences between the  
717 individual streamgage calibration and grouped calibration, Figure 13 illustrates that the grouped  
718 calibration strategy, which focused only on sensitive parameters, can provide just as much  
719 information as the individual streamgage calibration with no constraints on the parameter  
720 optimization other than the default ranges. The MWBM is a simple hydrologic model as it has  
721 minimal parameters, which are conceptual in nature (not physically based). It may be that this  
722 type of model is best for regionalization when parameter sensitivity can be identified and HRU  
723 behavior can be classified by a small number of clearly defined spatial groups. More  
724 complicated models with many more interactive parameters may not respond as well to this  
725 simple type of regionalization; more parameters may lead to more parameter interaction and  
726 situations of equifinality which might confuse the analysis.

727 The adjustments of precipitation and temperature parameters for the individual streamgage  
728 calibrations accounted for local errors such as rain gage under catch of precipitation. In addition  
729 these climate adjustments also account for local anthropogenic effects on streamflow (e.g. dams,  
730 diversions) since streamgages were not screened for these effects prior to individual streamgage  
731 calibration. In the grouped streamgage calibrations, the same precipitation and temperature  
732 adjustments are applied at every streamgage within the calibration region, making these climate  
733 adjustments more of a regional adjustment and producing more of a ‘reference’ condition for  
734 each calibration region.

### 735 **5.2 Parameter sensitivities and dominant process**

736 The MWBM parameter sensitivities varied by hydroclimatic index (RR and RV) and across the  
737 CONUS (Fig. 3). The parameter sensitivity patterns give an indication of dominant hydrologic  
738 processes based on MWBM. The dominant process can be seasonal and MWBM performance  
739 may be enhanced by extending the use of SA along the temporal domain to identify and  
740 temporally vary the parameters that are seasonally important to the MWBM. For example, error  
741 in peak flow months is the primary cause for poor model performance in the Platte Headwaters  
742 (Fig. 9). For the Platte Headwaters, the final parameter set performed well for simulated Z-  
743 scores for the regionalized low- and median-flow conditions (Fig. 9a, July through April), but  
744 was not able to replicate measured mean monthly flows for May and June. In this case, the  
745 dominant processes controlling hydrologic behavior change with season and the parameters  
746 controlling the dominant response may have to change accordingly (Gupta et al., 2008; Reusser  
747 et al., 2011).

### 748 **5.3 Model accuracy**

749 The pattern of MWBM accuracies shown in Fig. 8 and 14 are similar to those shown by Newman  
750 et al. (2015; Fig. 5a) in which a daily time-step hydrologic model was calibrated for 671 basins  
751 across the CONUS. Our study and the Newman et al. (2015) study both indicate the same  
752 ‘problem areas’ with the poorest performing basins generally being located in the high plains and  
753 desert southwest. Newman et al. (2015) attributed variation in model performance by region to

754 spatial variations in aridity and precipitation intermittency, contribution of snowmelt, and runoff  
755 seasonality.

756 The inferior MWBM results in the ‘problem areas’ can be attributed to multiple factors which  
757 likely include inadequate hydrologic process representation and errors in forcing data (e.g.  
758 climate data), and/or measured streamflow. Archfield et al. (2015) state that the performance of  
759 continental-domain hydrologic models is considerably constrained by inadequate model  
760 representation of dominant hydrologic processes. For example, the simplicity of the MWBM  
761 presents limitations on the representation of deeper groundwater reservoirs, gaining and losing  
762 stream reaches, simplistic AET, and the effects of surface processes (infiltration and overland  
763 flow) that need to be represented at finer time steps than monthly.

764 The dominant hydrologic processes in the ‘problem areas’ appear to be poorly represented at the  
765 daily (Newman et al., 2015) and monthly time steps. This may be due to inadequate forcing  
766 data, the quality of which ‘is paramount in hydrologic modeling efforts’ (Archfield et al., 2015)  
767 and/or the lack of ‘good’ reference streamflow data for calibration and evaluation. Both surely  
768 play a role and emphasize the need for incorporation of additional datasets so that calibration and  
769 evaluation of intermediate states in the hydrologic cycle are examined.

## 770 **Conclusions**

771 A parameter regionalization procedure was developed for the CONUS that transferred parameter  
772 values from gaged to ungaged areas for a MWBM. The FAST global-sensitivity algorithm was  
773 implemented on a MWBM to generate parameter sensitivities on a set of 109,951 HRUs across  
774 the CONUS. The parameter sensitivities were used to group the HRUs into 110 calibration  
775 regions. Streamgages within each calibration region were used to calibrate the MWBM  
776 parameters to produce a regionalized set of parameters for each calibration region. The  
777 regionalized MWBM parameter sets were used to simulate monthly runoff for the entire  
778 CONUS. Results from this study indicate that regionalized parameters can be used to produce  
779 satisfactory MWBM simulations in most parts of the CONUS.

780 The best MWBM results were achieved simulating low- and median-flows across the CONUS.  
781 The high-flow months generally showed lower skill levels than the low- and median-flow

782 months, especially for regions with dominant seasonal cycles. The lowest MWBM skill levels  
783 were found in the high plains and desert southwest and can be attributed to multiple factors  
784 which likely include inadequate hydrologic process representation and errors in forcing data  
785 and/or measured streamflow. Calibration and evaluation of intermediary fluxes and states in the  
786 MWBM through additional measured datasets may help to improve MWBM representations of  
787 these model states by helping to constrain parameterization to measured values.

788 **Acknowledgments**

789 This research was financially supported by the U.S. Department of Interior South Central  
790 Climate Science Center (<http://southcentralclimate.org/>), U.S. Environmental Protection Agency  
791 Office of Water, and the U.S. Geological Survey WaterSMART initiative. This paper is a  
792 product of discussions and activities that took place at the USGS John Wesley Powell Center for  
793 Analysis and Synthesis (<https://powellcenter.usgs.gov/>). Further project support was provided  
794 by the Jeff Falgout of the USGS Core Science Systems (CSS) Mission Area. Any use of trade,  
795 product, or firm names is for descriptive purposes only and does not imply endorsement by the  
796 U.S. Government.

797

798

799

800

801

802

803

804

805

806

807

808

809 **References**

- 810 Adam, J.C., and Lettenmaier, D.P.: Bias correction of global gridded precipitation for solid  
811 precipitation undercatch, *J. Geophys. Res.*, 108, 1-14, doi:10.1029/2002JD002499, 2003.
- 812 Ali, G., Tetzlaff, D., Soulsby, C., McDonnell, L.L., and Capell, R.: A comparison of similarity  
813 indices for catchment classification using a cross-regional dataset, *Adv. Water Resources*, 40,  
814 11-22, doi:10.1016/j.advwatres.2012.01.008, 2012.
- 815 Archfield, S.A., Clark, M., Areheimer, B., Hay, L.E., McMillan, H., Kiang, J.E., Seibert, J.,  
816 Bock, A., Wagener, T., Farmer, W.H., Andressian, V., Attinger, S., Viglione, A., Knight, R.,  
817 Markstrom, S., and Over, T.: Accelerating advances in continental domain hydrologic modeling,  
818 *Water Resour. Res.*, 51, 10078-10091, doi:10.1002/2015WR017498, 2015, .
- 819 Arnold, J.G., Moriasi, D.N., Gassman, P.W., Abbaspour, K.C., White, M.J., Srinivasan, R.,  
820 Santhi, C., Harmel, R.D., van Griensven, A., Van Liew, M.W., Kannan, N., and Jha, M.K.:  
821 SWAT: Model Use, Calibration and Validation, *T. ASABE*, 55(4), 1491-1508, 2012.
- 822 Blasone, R.-S., Madsen, H., and Rosbjerg, D.: Parameter estimation in distributed hydrological  
823 modelling: comparison of global and local optimisation techniques, *Nord. Hydrol.*, 34,451-476,  
824 doi:10.2166/nh.2007.024, 2007.
- 825 Blodgett, D.L., Booth, N.L., Kunicki, T.C., Walker, J.L., and Viger, R.J.: Description and  
826 Testing of the Geo Data Portal: A Data Integration Framework and Web Processing Services for  
827 Environmental Science Collaboration. US Geological Survey, Open-File Report 2011-1157, 9  
828 pp., Middleton, WI, USA, 2011.
- 829 Blöschl, G., and Sivapalan, M.: Scale issues in hydrological modeling: a review, *Hydrol.*  
830 *Process.*, 9, 251-290, 1995.
- 831 Blöschl, G., Sivapalan, M., Wagener, T., Viglione, A., and Savenije, H (Eds.): *Runoff Prediction*  
832 *in Ungauged Basins: Synthesis across Processes, Places, and Scales*. Cambridge University  
833 Press, Cambridge, England, 2013.

**Comment [Bock9]:** Updated this reference with the published information



834 Clark, M.P., and Slater, A.G.: Probabilistic Quantitative Precipitation Estimation in Complex  
835 Terrain, *B. Am. Meteorol. Soc.*, 7, 3-2, doi: [10.1175/JHM474.1](https://doi.org/10.1175/JHM474.1), 2006.

836 Cukier, R.I., Fortuin, C.M., Shuler, K.E., Petschek, A.G, and Schaibly, J.H: Study of sensitivity  
837 of coupled reaction systems to uncertainties in rate coefficients 1, *J. Chem. Phys.*, 59(8), 3873-  
838 3878, 1973.

839 Cukier, R.I., Schiably, J.H., and Shuler, K.E: Study of sensitivity of coupled reaction systems to  
840 uncertainties in rate coefficients 3, *J. Chem. Phys.*, 63(3), 1140-1149, 1975.

841 Cuo, L., Giambelluca, T.W., and Ziegler, A.D: Lumped parameter sensitivity analysis of a  
842 distributed hydrological model within tropical and temperate catchments, *Hydrol. Process.*,  
843 25(15), 2405-2421, doi:10.1002/hyp.8017, 2011.

844 Duan, Q., Gupta, V.K., and Sorooshian, S.: A shuffled complex evolution approach for effective  
845 and efficient optimization, *J. Optimiz. Theory App.*, 76, 501-521, doi:10.1007/BF00939380,  
846 1993.

847 Falcone, J.A., Carlisle, D.M., Wolock, D.M., and Meador, M.R.: GAGES: A stream gage  
848 database for evaluating natural and altered flow conditions in the conterminous United States,  
849 *Ecology*, 91, p. 621, A data paper in *Ecological Archives E091-045-D1*, available at  
850 <http://esapubs.org/Archive/ecol/E091/045/metadata.htm> (last accessed 15 November 2012),  
851 2010.

852 Farnsworth, R.K., Thompson, E.S., and Peck, E.L.: Evaporation Atlas for the Contiguous 48  
853 United States, NOAA Technical Report NWS 33, 41 pp., National Oceanic and Atmospheric  
854 Administration, Washington, D.C., 1982.

855 Groisman, P.Y., and Legates, D.R.: The accuracy of United States precipitation data, *Bull. Am.*  
856 *Meteorol. Soc.*, 75(2), 215-227, doi:10.1029/1998JD200110, 1994.

857 Gupta, H.V., Wagener, T., Liu, Y.Q.: Reconciling theory with observations: Elements of  
858 diagnostic approach to model evaluation, *Hydrol. Process.*, 22(18), 3802-3813,  
859 doi:10.1002/hyp.6989 .

860 Guse, B., Reusser, D.E., and Fohrer, N.: How to improve the representation of hydrological  
861 processes in SWAT for a lowland catchment - temporal analysis of parameter sensitivity and  
862 model performance, *Hydrol. Process.*, 28(4), 2561-2670, doi:10.1002/hyp.9777, 2013.

863 Hay, L.E., Leavesley, G.H., Clark, M.P., Markstrom, S.L., Viger, R.J., and Umemoto, M.: Step-  
864 wise multiple-objective calibration of a hydrologic model for a snowmelt-dominated basin, *J.*  
865 *Am. Water Resour. A.*, 42(4), 877-890, doi:10.1111/j.1752-1688.2006.tb04501.x, 2006.

866 Hay, L.E., and McCabe, G.J.: Spatial Variability in Water-Balance Model Performance in the  
867 Conterminous United States, *J. Am. Water Resour. Assoc.*, 38(3), 847-860, doi: 10.1111/j.1752-  
868 1688.2002.tb01001.x, 2002.

869 Hay, L.E., and McCabe, G.J.: Hydrologic effects of climate change in the Yukon River Basin,  
870 *Climate Change*, 100, 509-523, doi:10.1007/s10584-010-9805-x, 2010.

871 Kapangaziwiri, E., Hughes, D. A., and Wagener, T.: Constraining uncertainty in hydrological  
872 predictions for ungauged basins in southern Africa, *Hydrol. Sci. J.*, 57, 1000–1019, 5  
873 doi:10.1080/02626667.2012.690881, 2012.

874 Kiang, J.E., Stewart, D.W., Archfield, S.A., Osborne, E.B., and Eng, K.: A National Streamflow  
875 Network Gap Analysis. U.S. Geological Survey, Scientific Investigative Reports 2013-5013, 94  
876 pp., Reston, VA, USA, 2013.

877 Kirchner, J.W.: Getting the right answers for the right reasons: Linking measurements,  
878 analyses, and models to advance the science of hydrology, *J. Hydrol.*, 42, W03S04,  
879 doi:10.1029/2005WR004362, 2006.

880 Kokkonen, T.S., Jakeman, A.J., Young, P.C., and Koivusalo, H.J.: Predicting daily flows in  
881 ungauged catchments: model regionalization from catchment descriptors at the Coweeta  
882 Hydrologic Laboratory, North Carolina, *Hydrol. Process.*, 17, 2219-2238, doi:10.1002/hyp.1329,  
883 2003.

884 Krause, P., Doyle, D. P., and Bäse, F.: Comparison of different efficiency criteria for  
885 hydrological model assessment, *Adv. Geosci.*, 5, 89–97, doi:10.5194/adgeo-5-89-2005, 2005.

886 Legates, D.R., and McCabe,G.J.: Evaluating the use of “goodness-of-fit” Measures in  
887 hydrologic and hydroclimatic model validation, *Water Resour. Res.*, 35(1), 233-241,  
888 doi:10.1029/1998WR900018, 1999.

889 Maurer, E.P., Wood, A.W., Adam, J.C., Lettenmaier, D.P., and Nijseen, B.: A long-term  
890 hydrologically-based data set of land surface fluxes and states for the conterminous United  
891 States, *J. Climatol.*, 15, 3237-3251, doi:10.1175/1520-  
892 0442(2002)015<3237:ALTHBD>2.0.CO;2, 2002.

893 McCabe, G.J., Hay, L.E., Bock, A., Markstrom, S.L., and Atkinson, D.R.: Inter-annual and  
894 spatial variability of Hamon potential evapotranspiration model coefficients, *J. Hydrol.*, 521,  
895 389-394, doi:10.1016/j.jhydrol.2014.12.006, 2015.

896 McCabe, G.J., and Markstrom, S.L.: A Monthly Water-Balance Model Driven By a Graphical  
897 User Interface. U.S. Geological Survey Open-File Report 2007-1008, 12 pp., Reston, VA, USA,  
898 2007.

899 McCabe, G.J., and Wolock, D.M.: Century-scale variability in global annual runoff examined  
900 using a water balance model, *Int. J. Climtol.*, 31, 1739-1748, doi:10.1002/joc.2198, 2011a.

901 McCabe, G.J., and Wolock, D.M.: Independent effects of temperature and precipitation on  
902 modeled runoff in the conterminous United States, *Water Resour. Res.*, 47, W1152,  
903 doi:10.1029/2011WR010630, 2011b.

904 McManamay, R.A., Orth, D.J., Dolloff, C.A., and Frimpong, E.A: Regional Frameworks  
905 applied to Hydrology: Can Landsapes-based frameworks capture the hydrologic variability?,  
906 *River Res. App.*, 28, 1325-1339, doi:10.1002/rra.1535, 2011.

907 Merz, R., and Blöschl, G.: Regionalisation of catchment model parameters, *J. Hydrol.*, 287, 95-  
908 123, doi:10.1016/j.jhydrol.2003.09.028, 2004.

909 Moriasi, D.N, Arnold, J.G., Van Liew, M.W., Bingner, R.L., Harmel, R.D., and Vieth, T.L.:  
910 Model Evaluation Guidelines for Systematic Quantification of Accuracy in Watershed  
911 Simulations, *T. ASABE*, 50, 885-900, 2007.

912 Nash, J.E., and Sutcliffe, J.V.: River flow forecasting through conceptual models Part I: a  
913 discussion of principles, *J. Hydrol.*, 10, 282-290, doi:10.1016/0022-1694(70)90255-6, 1970.

914 National Operational Hydrologic Remote Sensing Center, Snow data Assimilation System  
915 (SNODAS) Data Products at the NSIDC, 9/30/2003 through 6/13/2014, National Snow and Ice  
916 Data Center, Boulder, Colorado, USA, doi:10.7265/N5TB14TC, 2004.

917 Newman, A.J., Clark, M.P., Sampson, K., Wood, A., Hay, L.E., Bock, A., Viger, R.J., Blodgett,  
918 D., Brekke, L., Arnold, J.R., Hopson, T., and Duan, Q.: Development of a large-sample  
919 watershed-scale hydrometeorological data set for the contiguous USA: data set characteristics  
920 and assessment of regional variability in hydrologic model performance, *Hydrol. Earth Syst. Sc.*,  
921 19, 209-223, doi:10.5194/hess-19-209-2015, 2015.

922 Oudin, L., Andreassian, V., Perrin, C., Michel, C., and Le Moine, N.: Spatial proximity,  
923 physical similarity, regression and ungauged catchments: a comparison of regionalization  
924 approaches based on 913 French catchments, *Water Resour. Res.*, 44, 1-15,  
925 doi:10.1029/2007WR006240, 2008.

926 Oudin, L., Kay, A., Andreassian, V., and Perrin, C.: Are seemingly physically similar  
927 catchments truly hydrologically similar?, *Water Resour. Res.*, 46, W11558,  
928 doi:10.1029/2009WR008887, 2010.

929 Oyler, J.W., Dobrowski, S.Z., Ballantyne, A.P., Klene, A.E., and Running, S.W.: Artificial  
930 amplification of warming trends across the mountains of the western United States, *Geophys.*  
931 *Res. Lett.*, 42, 153-161, doi:10.1002/2014GL062803, 2015.

932 Peel, M.C., Chiew, F.H.S., Western, A.W., and McMahon, T.A.: Extension of unimpaired  
933 monthly streamflow data and regionalization of parameter values to estimate streamflow in  
934 ungauged catchments. Report to National Land and Water Resources Audit, Center for  
935 Environmental Application and Hydrology, University of Melbourne, Parkville, 2000.

936 R Core Team: R: A language and environment for statistical computing, R Foundation for  
937 Statistical Computing, Vienna, Austria, 2013.

938 Reusser, D.: fast: Implementation of the Fourier Amplitude Sensitivity Test (FAST), R package  
939 version, <http://CRAN.R-project.org/package=fast>, (last access: 9 April 2014), 2012.

940 Reusser, D., Buytaert, W., and Zehe, E.: Temporal dynamics of model parameter sensitivity for  
941 computationally expensive models with the Fourier amplitude sensitivity test, *Water Resour.*  
942 *Res.*, 47, W07551, doi:10.1029/2010WR009947, 2011.

943 Saltelli, A., Tarantola, S., and Campolongo, F.: Sensitivity analysis as an ingredient of  
944 modeling, *Stat. Sci.*, 15, 377-395, 2000.

945 Samuel, J., Coulibaly, P., and Metcalfe, R.A.: Estimation of Continuous Streamflow in Ontario  
946 Ungauged Basins: Comparison of Regionalization Methods, *J. Hydrol. Eng.*, 16, 447-459,  
947 doi:10.1061/(ASCE)HE.1943-5584.0000338, 2011.

948 Sankarasubramanian, A., and Vogel, R.M.: Hydroclimatology of the continental United States,  
949 *Geophys. Res. Lett.*, 30, 1-4, doi:10.1029/2002GL015937, 2003.

950 Santhi, C., Kannan, N., Arnold, J.G., and Luzio, D.: Spatial calibration and temporal validation  
951 of flow for regional scale hydrologic modeling, *J. Am. Water Resour. Assoc.*, 4, 829-846,  
952 doi:10.1111/j.1752-1688.2008.00207.x, 2008.

953 Sawicz, K., Wagener, T., Sivapalan, M., Troch, P.A., and Carrillo, G.: Catchment classification:  
954 empirical analysis of hydrologic similarity based on catchment function in the eastern USA,  
955 *Hydrol. Earth Syst. Sc.*, 15, 2895-2911, 2011.

956 Sefton, C.E.M., and Howarth, S.M.: Relationships between dynamic response characteristics  
957 and physical descriptors of catchments in England and Wales, *J. Hydrol.*, 211, 11-16,  
958 doi:10.1016/S0022-1694(98)00163-2, 1998.

959 Seibert, J.: Regionalization of parameters for a conceptual rainfall runoff model, *Agr. Forest*  
960 *Meteorol.*, 98-99, 279-293, doi:10.1016/S0168-1923(99)00105-7, 1999.

961 Smakhtin, V.Y.: Low flow hydrology: a review, *J. Hydrol.*, 240, 147-186, doi:10.1016/S0022-  
962 1694(00)00340-1, 2001.

963 Tang, Y., Reed, P., Wagener, T., and van Werkhoven, T.: Comparing sensitivity analysis  
964 methods to advance lumped watershed model identification and evaluation, *Hydrol. Earth Syst.*  
965 *Sc.*, 11, 793-817, 2007.

966 Tekleab, S., Uhlenbrook, S., Mohamed, Y., Savenije, H.H.G., Temesgen, M., and Wenninger, J.:  
967 Water balance modeling of Upper Blue Nile catchments using a top-down approach, *Hydrol.*  
968 *Earth Syst. Sci.*, 15, 2179-2193, doi:10.5194/hess-15-2179-2011, 2011.

969 Troch, P.A., Paniconi, C., and McLaughlin, D.: Catchment-scale hydrological modeling and  
970 data assimilation, *Adv. Water Resour.*, 26, 131-135, doi:10.1016/S0309-1708(02)00087-8, 2003.

971 US Geological Survey: A National Water Information System, available at: <http://waterdata.usgs.gov/nwis/> (last access 27 March 2014), 2014.

973 Van Griensven, A., Meixner, T., Grunwald, S., Bishop, T., Diluzio, and M., Srinivasan, R.: A  
974 global sensitivity analysis tool for the parameters of multi-variable catchment models, *J. Hydrol.*,  
975 324, 10-23, doi:10.1016/j.jhydrol.2005.09.008, 2006.

976 Vandewiele, G.L., and Elias, A.: Monthly water balance of ungaged catchments obtained by  
977 geographical regionalization, *J. Hydrol.*, 170, 277-291, doi:10.1016/0022-1694(95)02681-E,  
978 1995.

979 Viger, R., Bock, A.: GIS Features of the Geospatial Fabric for National Hydrologic Modeling,  
980 U.S. Geological Survey, Denver, CO, USA, doi:10.5066/F7542KMD, 2014.

981 Vogel, R.M.: Regional calibration of watershed models, *Watershed Models*, Singh, V.P., and  
982 Frevert, D.F. (Eds.), CRC Press, Boca Raton, FL, USA, 2006.

983 Vrugt, J.A., ter Braak, C.J.F., Clark, M.P., Hyman, J.M., Robinson, B.A.: Treatment of input  
984 uncertainty in hydrologic modeling: Doing hydrology backwards with Markov Chain Monte  
985 Carlo simulation, *Water Resour. Res.*, 44, W00B09, doi:10.1029/2007WR006720, 2008.

986 Wolock, D.M.: STATSGO soil characteristics for the conterminous United States. U.S.  
987 Geological Survey Open-File Report 1997-656, Reston, VA, USA, available at:  
988 <http://water.usgs.gov/GIS/metadata/usgswrd/XML/muid.xml>, (last access 3 March 2012), 1997.

989 Wolock, D.M., and McCabe, G.J.: Explaining spatial variability in mean annual runoff in the  
990 conterminous United States, *Clim. Res.*, 11, 149-159, doi:10.3354/cr011149, 1999.

991 Zhang, X., Srinivasan, R., and Van Liew, M.: Multi-Site Calibration of the SWAT Model for  
992 Hydrologic Modeling, *T. ASABE*, 51, 2039-2049, 2008.

993

994

995

996

997

998

999

1000

1001

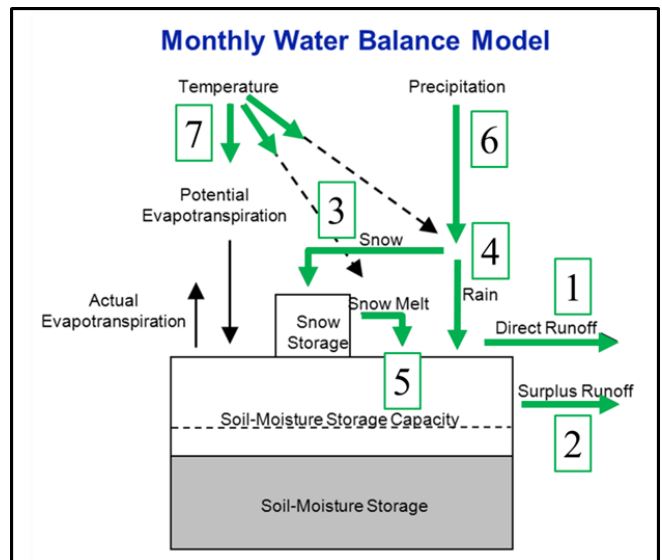
1002

Parameter	Definition	Range	Default
<b>1. <i>Drofac</i></b>	Controls fraction of precipitation that becomes runoff	0, 0.10	0.05
<b>2. <i>Rfactor</i></b>	Controls fraction of surplus that becomes runoff	0.10, 1.0	0.5
<b>3. <i>Tsnow</i></b>	Threshold above which all precipitation is	-10.0, -2.0	-4.0

	rain ( $^{\circ}\text{C}$ )		
4. <i>Train</i>	Threshold below which all precipitation is snow ( $^{\circ}\text{C}$ )	0.0, 10.0	7.0
5. <i>Meltcoef</i>	Proportion of snowpack that becomes runoff	0.0, 1.0	0.47
6. <i>Ppt_adj</i>	Seasonal adjustment factor for precipitation (%)	0.5, 2.0	1
7. <i>Tav_adj</i>	Seasonal adjustment for temperature ( $^{\circ}\text{C}$ )	-3.0, 3.0	0

1003  
1004  
1005  
1006  
1007  
1008  
1009

Table 1. Monthly Water Balance Model parameters and ranges.



1010



1011 Figure 1. Conceptual diagram of the Monthly Water Balance Model (McCabe and Markstrom  
1012 2007). Processes influenced by model parameters used in Fourier Amplitude Sensitivity Test  
1013 (FAST) those identified by green arrow and numbered 1-5 (Table 1).

1014

1015

1016

1017

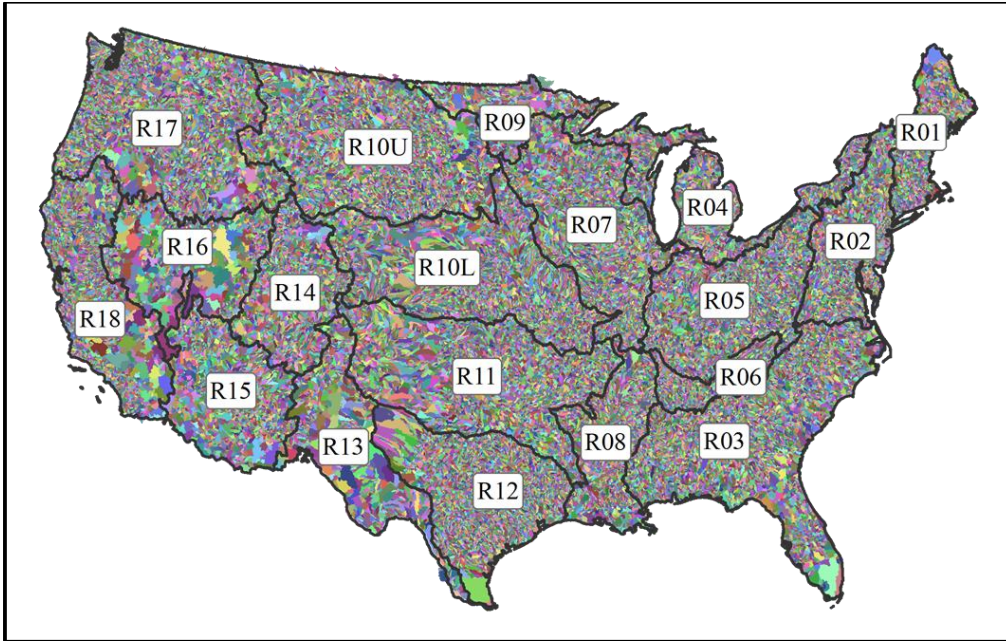
1018

1019

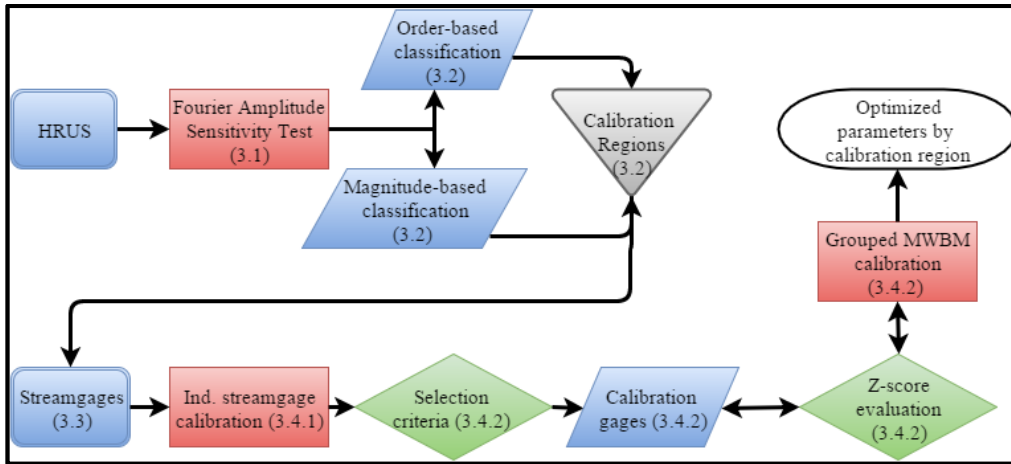
1020

1021

1022



1023  
 1024 Figure 2. Hydrologic Response Units of the Geospatial Fabric, differentiated by color, overlain  
 1025 by NHDPlus region boundaries (R01-R18).



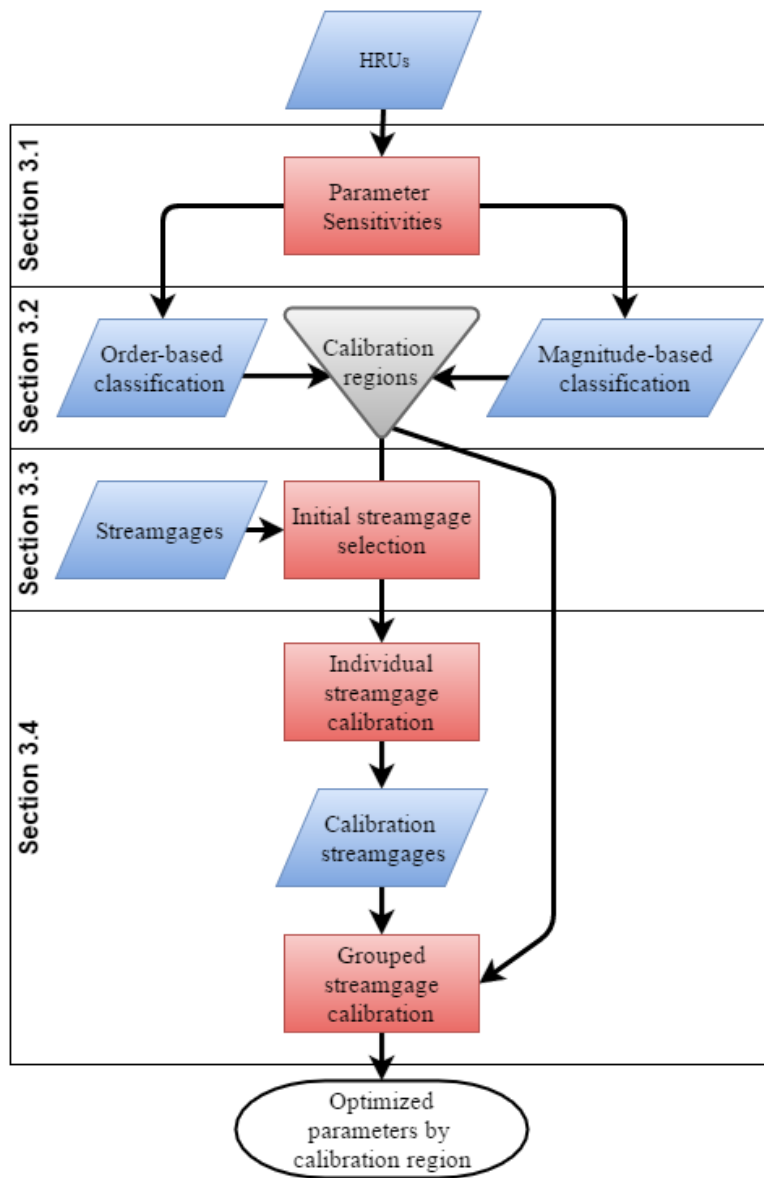
Comment [Bock10]: Removed this older flow chart in favor of the updated one.

1026  
 1027

1028

1029

1030



**Comment [Bock11]:** Based on reviewer comments #3, I created a new flow chart that more closely matches both the order of operations and language of Section 3

1031

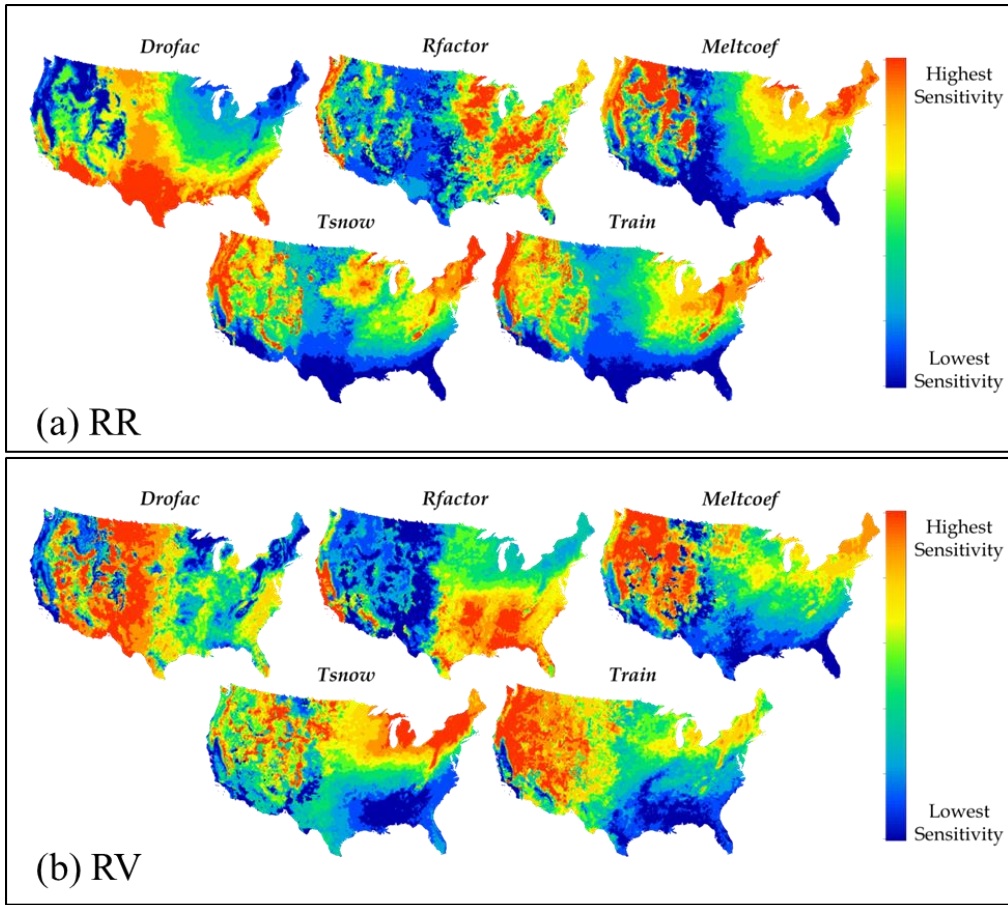
1032

1033

1034

*Figure 3. Schematic flowchart of the parameter regionalization procedure described in Section 3: Parameter sensitivities (3.1), Calibration regions (3.2), Initial streamgage selection (3.3), and Grouped streamgage calibration (3.4).*

**Comment [Bock12]:** Modified caption for figure 3 to add more description



1035

1036

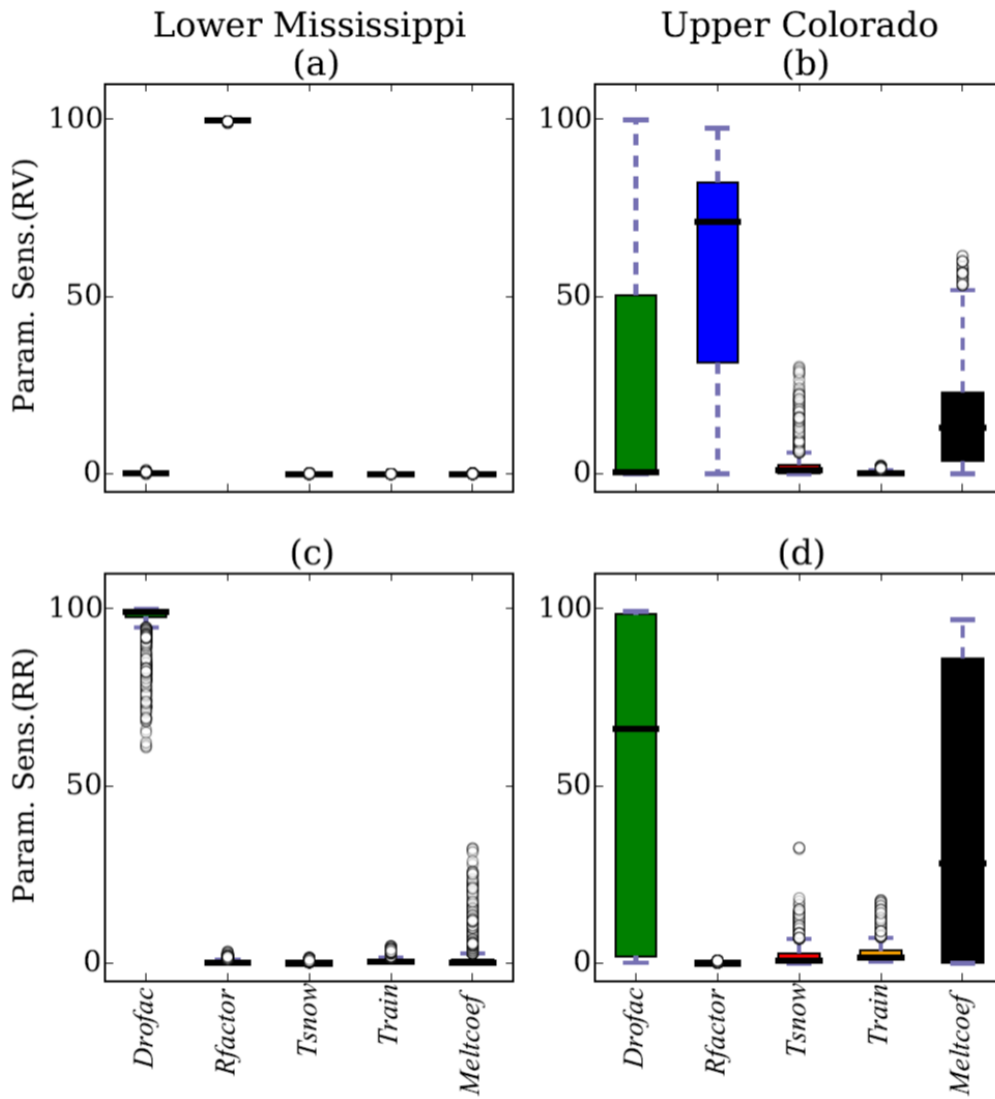
1037

1038

1039

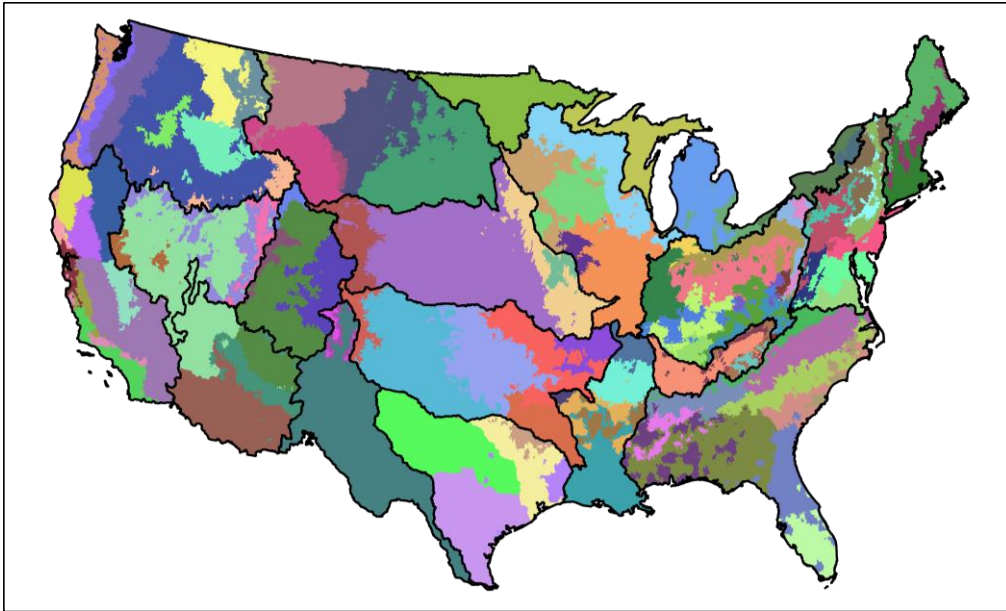
1040

Figure 4. Relative sensitivity of the (a) Rainfall Ratio (RR) and (b) Runoff Variability (RV) indices to Monthly Water Balance Model parameters.



1041 Figure 5. Parameter sensitivities of Runoff Variability (RV; a and b) and Runoff Ratio (RR; c  
 1042 and d) indices for Monthly Water Balance Model parameters in the Lower Mississippi (R08) and  
 1043 Upper Colorado (R14).  
 1044

1045



1046

1047

Figure 6. Final 110 Monthly Water Balance Model calibration regions differentiated by colors.

1048

A subset of streamgages within each calibration region were calibrated in a group-wise fashion

1049

to produce a single optimized parameter set for the entire region (Fig. 3).

1050

1051

1052

1053

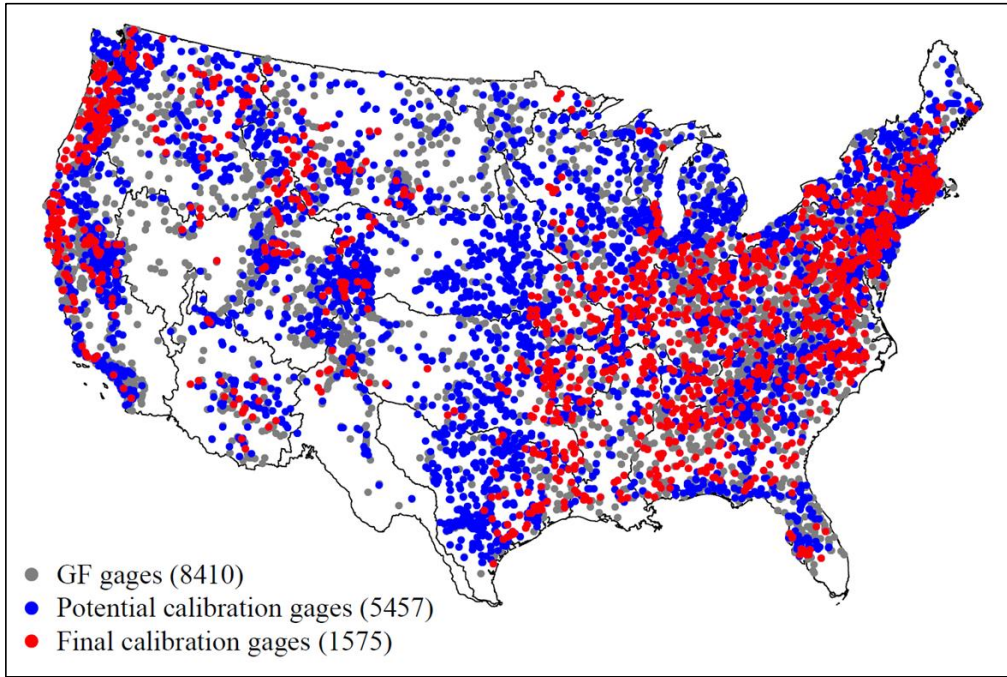
1054

1055

1056

1057

1058



1059

1060 Figure 7. Streamgages tested in the study. GF notes geospatial fabric for national hydrologic  
1061 modeling (Viger and Bock, 2014).

1062

1063

1064

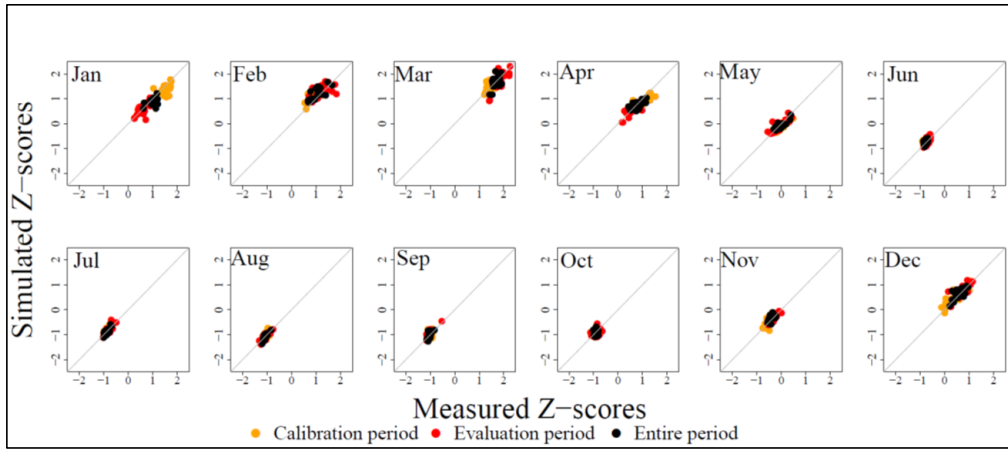
1065

1066

1067

1068





1069

1070 Figure 8. Measured versus simulated mean monthly Z-scores for the Tennessee River calibration  
 1071 region (see Fig. 9b for location). Orange is calibration, red is evaluation, and black is all years.

1072

1073

1074

1075

1076

1077

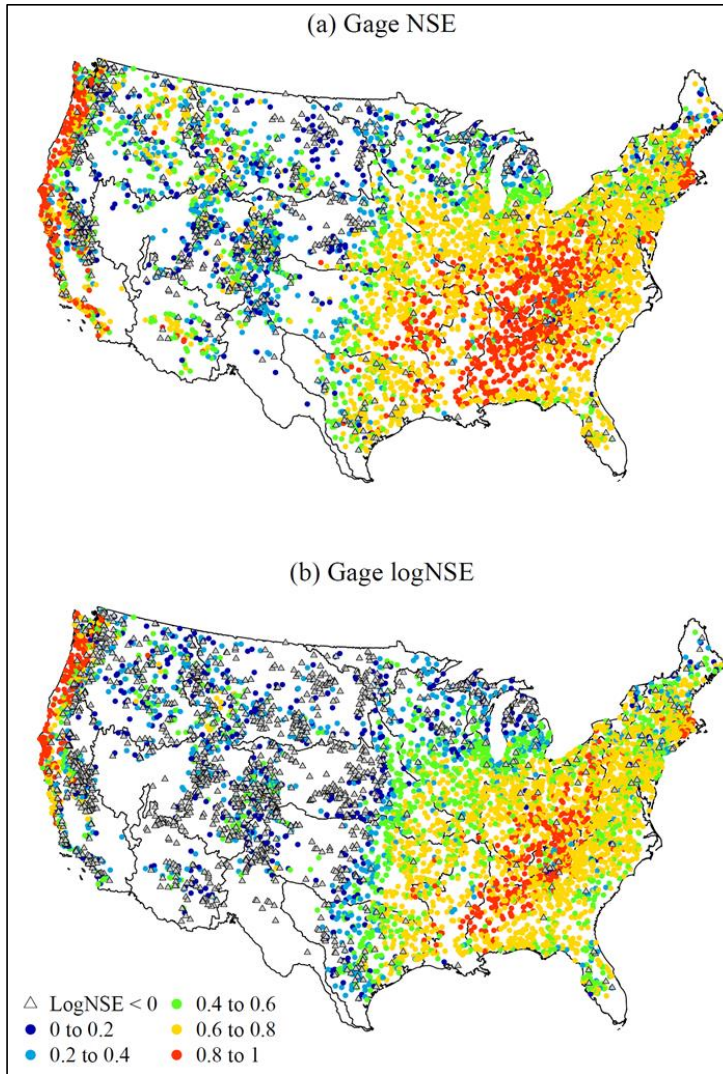
1078

1079

1080

1081

1082

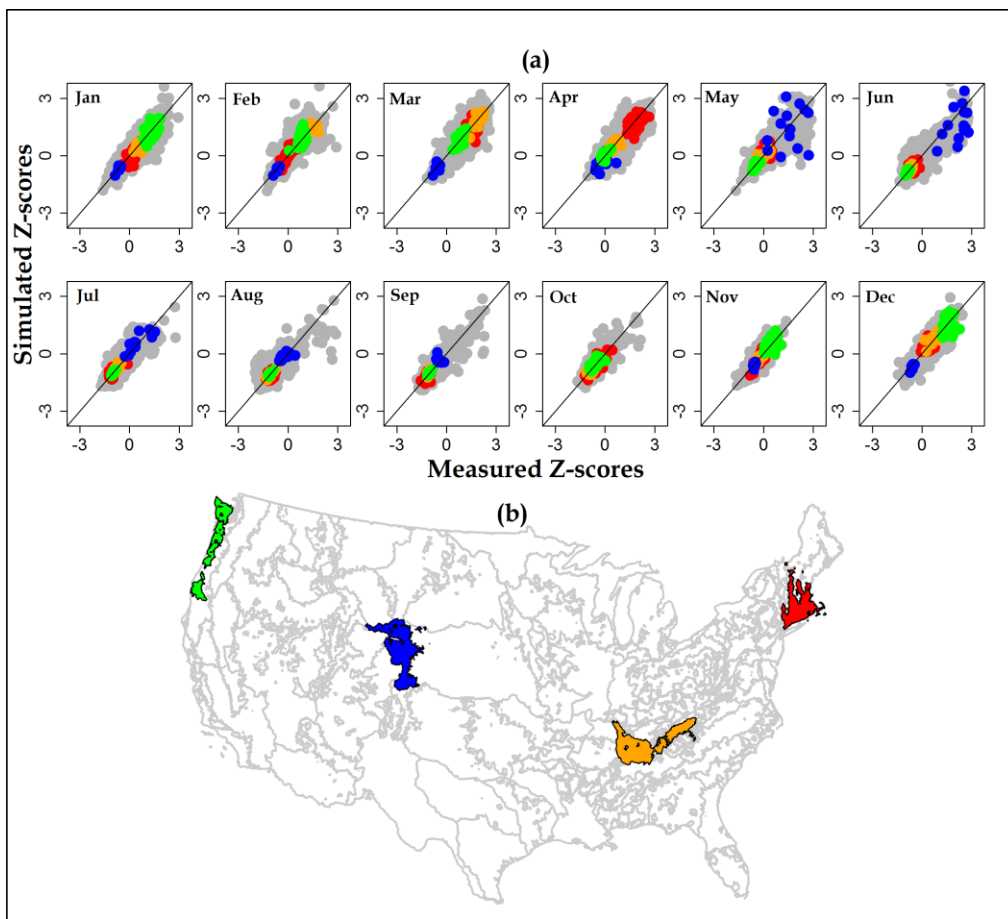


1083

1084 Figure 9. Individual streamgage calibration results: (a) Nash-Sutcliffe Efficiency (NSE)  
 1085 coefficient and (b) log of the NSE (logNSE).

1086

1087

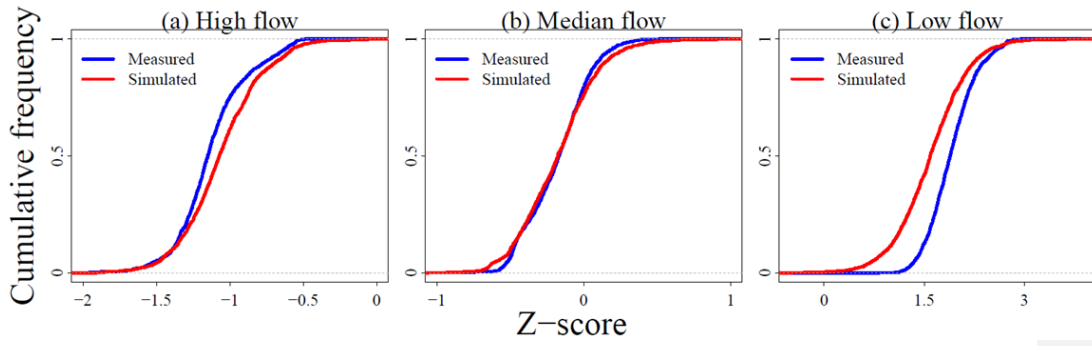


1088  
 1089 Figure 10. (a) Measured versus simulated mean monthly Z-scores for runoff at all streamgages  
 1090 and (b) location of highlighted streamgages for four calibration regions: New England (67  
 1091 streamgages, red); Tennessee River (21 streamgages, orange); Platte Headwaters (15  
 1092 streamgages, blue); and Pacific Northwest (33 streamgages, green).

1093

1094

1095



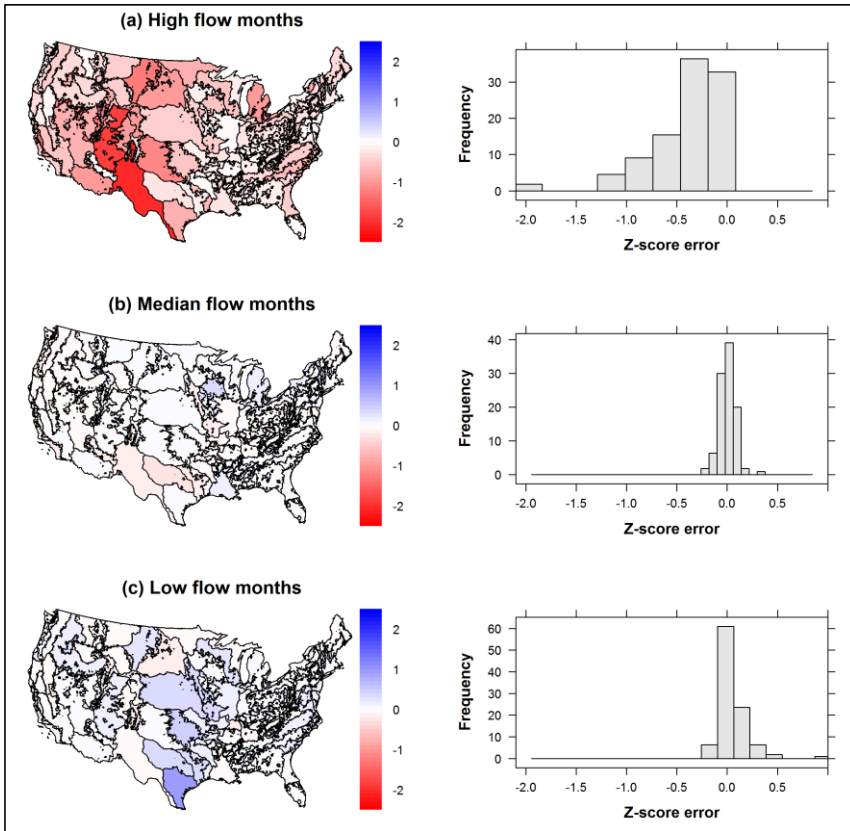
1096

1097 Figure 11. Z-score cumulative frequency for (a) highest-, (b) median-, and (c) lowest-flow

1098

months.

1099



1100

1101

1102

1103

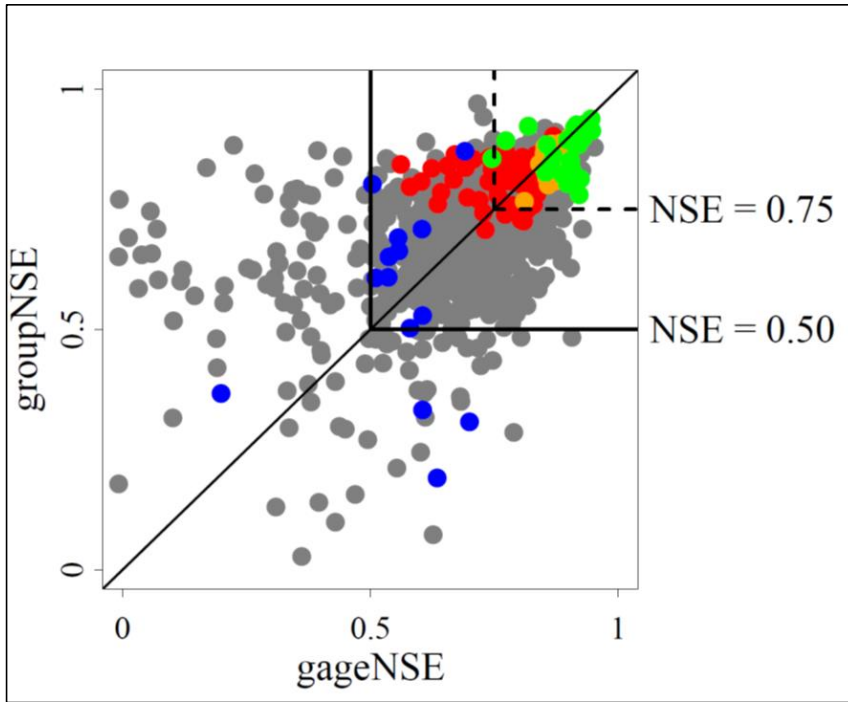
1104

1105

1106

1107

Figure 12. Z-score error (simulated - measured) for (a) highest-, (b) median-, and (c) lowest-flow months.



1108

1109

1110

1111

1112

1113

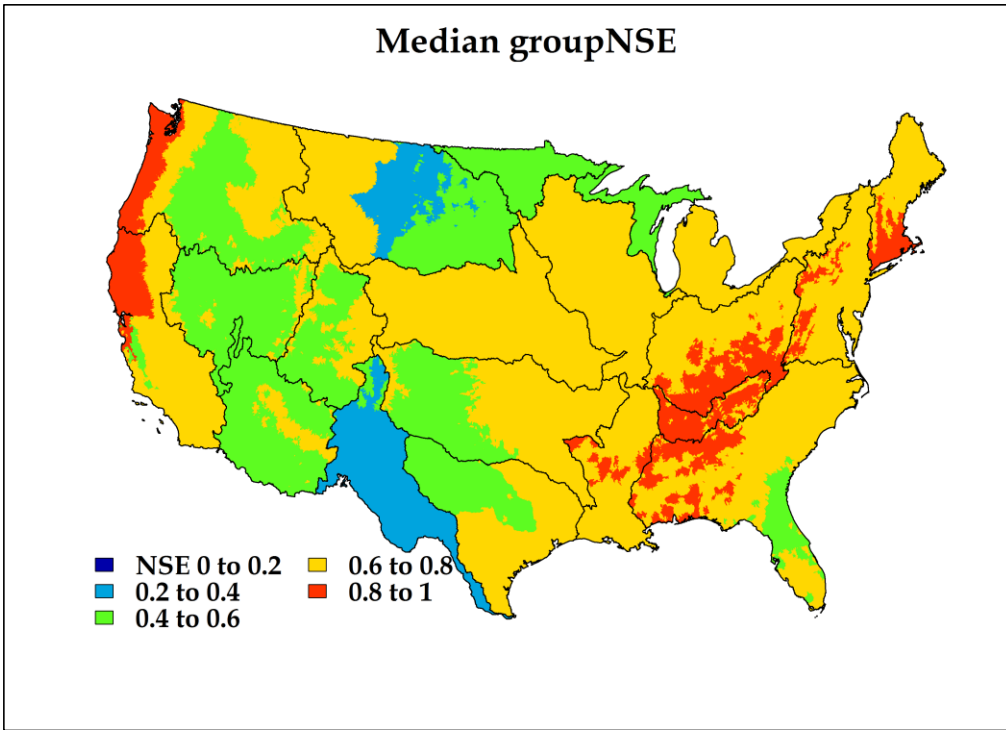
1114

1115

1116

1117

Figure 13. Nash Sutcliffe Efficiency from individual (gageNSE) and grouped (groupNSE) calibration. Calibration regions in New England (67 streamgages, red); Tennessee River (21 streamgages, orange); Platte Headwaters (15 streamgages, blue); and Pacific Northwest (33 streamgages, green) are highlighted (see Fig. 9b for location).



1118

1119 Figure 14. Median Nash Sutcliffe Efficiency (NSE) of streamgages used for calibration by  
 1120 calibration region.

1121

1122

1123

1124

1125

1126

1127

1128

1129